

Muonic Force Behind Flavor Anomalies

Admir Greljo,¹ Yotam Soreq,² Peter Stangl,¹ Anders Eller Thomsen,¹ Jure Zupan³

¹*Albert Einstein Center for Fundamental Physics, Institute for Theoretical Physics, University of Bern, CH-3012 Bern, Switzerland*

²*Physics Department, Technion – Israel Institute of Technology, Haifa 3200003, Israel*

³*Department of Physics, University of Cincinnati, Cincinnati, Ohio 45221, USA*

E-mail: admir.greljo@unibe.ch, soreq@physics.technion.ac.il,
stangl@itp.unibe.ch, thomsen@itp.unibe.ch, zupanje@ucmail.uc.edu

ABSTRACT: We develop an economical theoretical framework for combined explanations of the flavor physics anomalies involving muons: $(g - 2)_\mu$, $R_{K^{(*)}}$, and $b \rightarrow s\mu^+\mu^-$ angular distributions and branching ratios, that was first initiated by some of us in Ref. [1]. The Standard Model (SM) is supplemented with a lepton-flavored $U(1)_X$ gauge group. The $U(1)_X$ gauge boson with the mass of $\mathcal{O}(0.1)$ GeV resolves the $(g - 2)_\mu$ tension. A TeV-scale leptoquark, charged under the $U(1)_X$, carries a muon number and mediates B -decays without prompting charged lepton flavor violation or inducing proton decay. We explore the theory space of the chiral, anomaly-free $U(1)_X$ gauge extensions featuring the above scenario, and identify 273 suitable charge assignments for the $SM+3\nu_R$ fermion content with the integer charges in the range $X_{F_i} \in [-10, 10]$. We then carry out a comprehensive phenomenological study of the muonic force in representative benchmark models. Interestingly, a large class of models can resolve the tension without conflicting the complementary constraints, and all of the viable parameter space will be tested in future muonic resonance searches. Finally, the catalog of the anomaly-free lepton-non-universal charge assignments motivated us to explore different directions in model building. We present a model in which the muon mass and the $(g - 2)_\mu$ are generated radiatively from a common short-distance dynamics after the $U(1)_X$ breaking. We also show how to charge a vector leptoquark under $U(1)_{\mu-\tau}$ in a complete gauge model.

Contents

1	Introduction	2
2	Model classification	4
2.1	General gauged flavor $U(1)_X$	4
2.2	Quark flavor universal $U(1)_X$	5
2.2.1	Vector category $U(1)_X$ charge assignments	7
2.2.2	Chiral category $U(1)_X$ charge assignments	9
3	Light X_μ phenomenology	10
3.1	Muon $(g-2)_\mu$	10
3.2	Neutrino trident production	11
3.3	Other constraints	12
3.4	A single mediator for both $(g-2)_\mu$ and rare B decay anomalies?	12
3.5	Benchmarks	15
3.5.1	Gauged $L_\mu - L_\tau$	16
3.5.2	Gauged $B - 3L_\mu$	17
3.5.3	Gauged $L_e - L_\mu$	17
3.5.4	Chiral models	18
4	Muon mass and $(g-2)_\mu$ at one loop	20
5	A vector muoquark model	23
6	Conclusions	25
A	Kinetic mixing	27
A.1	Equivalence of charge assignments	27
A.2	Mass basis of the gauge sector	28
A.3	The RG running of the kinetic mixing parameter	29
B	The X boson phenomenology	30
B.1	Neutrino trident limits	30
B.2	Decay channels	31
B.3	$R_{K^{(*)}}$ from a light X_μ vector boson	31
C	The generators of $U(1)$ embeddings in $SU(5)$	34

1 Introduction

Two sets of observables may be pointing to a new muonic force: *i*) that the measurements of the anomalous magnetic moment of the muon, $(g - 2)_\mu$, [2, 3] are disagreeing with the R -ratio data-driven theory prediction [3–24] (however, see also [25]) and *ii*) the deviations from predictions in rare B meson decay observables, in particular $b \rightarrow s\mu^+\mu^-$ angular distributions [26, 27] and branching ratios [28–32] (we will collectively refer to them as “ $b \rightarrow s\mu\mu$ anomalies”) and the lepton-flavor universality (LFU) ratios $R_{K^{(*)}}$ [33, 34]. Among these, the observables $R_{K^{(*)}}$ stand out in particular, because their predictions are extremely clean in the Standard Model (SM) [35–37]. The most recent update of R_K increased the significance of the anomaly and, for the first time, LHCb declared evidence for lepton flavor universality violation (LFUV) [34]. While $R_{K^{(*)}}$ could be explained by NP coupling to electrons or muons, an explanation in terms of muonic NP provides a consistent combined explanation of all anomalies in rare B decays, i.e. the $b \rightarrow s\mu\mu$ anomalies and $R_{K^{(*)}}$ (for recent global fits see e.g. [38–42]).

In contrast to the possible new flavor-diagonal couplings of New Physics (NP) to muons there is striking absence of any such NP hints in lepton-flavor-violating (LFV) transitions, such as $\mu \rightarrow e\gamma$ and $\mu \rightarrow 3e$. Numerically, taking as an example NP that induces the dimension-5 dipole moment operators after the electroweak symmetry breaking, $\mathcal{L}_{\text{eff}} \supset -e v \bar{\ell}_L^i \sigma^{\mu\nu} \ell_R^j F_{\mu\nu} / (4\pi\Lambda_{ij})^2 + \text{h.c.}$, with $v = 246$ GeV the electroweak vacuum expectation value (VEV), the NP scale required to explain the $(g - 2)_\mu$ anomaly is $\Lambda_{22} \simeq 15$ TeV. This should be compared with the much more stringent bound $\Lambda_{12(21)} \gtrsim 3600$ TeV on the effective NP scale implied by the absence of the $\mu \rightarrow e\gamma$ transition [43]. The hierarchy between the two effective scales persists even if the couplings to electrons are Yukawa suppressed: $\Lambda_{12(21)} \sqrt{m_e/m_\mu} \gtrsim 250$ TeV. Qualitatively similar implications follow from the absence of $\tau \rightarrow \mu\gamma$ transitions [44].

The high suppression of flavor-violating effects strongly hints at NP with an almost exact muon-number symmetry, $U(1)_{L_\mu}$. The $U(1)_{L_\mu}$ symmetry forbids flavor-violating transitions with muons, but still allows for deviations from flavor universality, i.e., different flavor-diagonal couplings to electrons, muons, and taus. A number of proposed solutions to the experimental anomalies are based on an anomaly-free lepton-flavored symmetry group $U(1)_{L_\mu-L_\tau}$ [45–54]. For instance, a light $U(1)_{L_\mu-L_\tau}$ gauge boson X_μ can generate a 1-loop contribution to $(g - 2)_\mu$ of the right size in order to explain the deviations in the experimental measurements, while at the same time not being excluded by the other searches [48, 49]. For the $R_{K^{(*)}}$ anomalies, on the other hand, a heavy gauge field X_μ was used, along with a set of vector-like quarks [53, 54]. The other gauging choices used to explain $R_{K^{(*)}}$ are $U(1)_{B_3-L_\mu}$ [55–57], third family hypercharge [58–60], and other alternatives [60–74]. Note, however, that it is not possible to explain both $(g - 2)_\mu$ and $R_{K^{(*)}}$ in an effective field theory (EFT) with a single light mediator X_μ that provides the dominant contribution. We show this in complete generality in Section 3.4: the size of the X_μ contribution required to explain the deviations in $(g - 2)_\mu$ and $R_{K^{(*)}}$ is ruled out by a combination of constraints from $B \rightarrow K\nu\bar{\nu}$, $\tau \rightarrow 3\mu$ and neutrino trident production.

A different class of mediators that can successfully explain the flavor anomalies are the

leptoquarks [75]. The lepton-flavored $U(1)_X$ gauge symmetry would constrain the leptoquark couplings, which can be crucial for having a viable phenomenology [1, 76, 77]. For instance, the TeV-scale *muoquarks*, i.e., the leptoquarks that interact only with muons and not with electrons or taus, are motivated by both *i*) the already mentioned muon anomalies in $(g-2)_\mu$ and rare B decays; and *ii*) by the stringent constraints on the charged LFV. A subset of chiral anomaly-free $U(1)_X$ extensions of the SM, under which leptoquarks are charged, provide natural theories for muoquarks while also addressing the absence of proton decay. A pragmatic proposal for the common explanation of the muon anomalies utilizes a light X_μ for $(g-2)_\mu$ and a heavy muoquark $S_3 = (\bar{\mathbf{3}}, \mathbf{3}, 1/3)_{8/3}$ connected by the underlying $U(1)_{B-3L_\mu}$ symmetry [1].

In this paper, we systematically explore the theory space of anomaly-free $U(1)_X$ gauge extensions of the SM, extending the scenario in Ref. [1]. In Section 2 we study the anomaly-cancellation conditions and identify a complete set of quark-flavor-universal $U(1)_X$ models with appropriate rational charge assignments for the SM+ $3\nu_R$ chiral fermions with the maximal charge ratios ≤ 10 . The solutions are classified as vector-like (Section 2.2.1) or chiral (Section 2.2.2) depending on the charges of the left- and the right-handed e , μ and τ .

We then address whether or not $U(1)_{L_\mu-L_\tau}$ and $U(1)_{B-3L_\mu}$ are the unique gauge groups that can lead to a successful phenomenology: the explanation of $(g-2)_\mu$ with the light X_μ while avoiding all other constraints. As we will show, there are numerous other anomaly-free gauge group choices that are not excluded by the present experimental constraints and can simultaneously explain the $(g-2)_\mu$ anomaly. We carry out a detailed phenomenological study to confront the preferred region (Section 3.1) with the complementary constraints from neutrino trident (Section 3.2), Borexino and light resonance searches (Section 3.3). The constraints are applied to several carefully chosen benchmark models in Section 3.5. The main phenomenological difference between the models is how the electron is charged under $U(1)_X$. As expected, models in which the electron is not charged under $U(1)_X$ pass the experimental constraints easily.

The lepton-flavored $U(1)_X$ systematics outlined in Section 2 opens up new directions in model building beyond the scenario of Ref. [1]. We illustrate this with two examples. In Section 4 we present a model in which the muon mass and the $(g-2)_\mu$ are both radiatively generated at one-loop level by the TeV-scale muoquarks after the $U(1)_X$ -breaking scalar obtains a VEV. This is made possible by the chiral solutions of the anomaly cancellation conditions, which forbid the dimension-4 muon Yukawa in the unbroken phase. Remarkably, the $(g-2)_\mu$ tension and the muon mass sharply predict the leptoquark mass in the range that is of interest for direct searches at colliders. A different type of a model building example is presented in Section 5, where we show how to construct an ultraviolet (UV) completion of the vector muoquark model. This example also gives a possible unification scenario of the $U(1)_X$ into a simple Lie group.

Finally, Section 6 contains our conclusions, while Appendices contain further details on the equivalence of charge assignments for the products of $U(1)$ subgroups (Appendix A.1), the mass basis of the gauge sector (Appendix A.2), the RG running of the kinetic mixing (Appendix A.3), the neutrino trident limits (Appendix B.1), the X boson decay channels (Appendix B.2), the contributions to $R_{K^{(*)}}$ from a light X vector boson (Appendix B.3)

and the generators of $U(1)_X$ embeddings in $SU(5)$ (Appendix C).

2 Model classification

We start by classifying the anomaly free models that, in addition to the SM, contain a new gauge group $U(1)_X$ and a muoquark, that is, a leptoquark that only couples to muon flavored fermions (muons and muon neutrinos). We assume that all the couplings allowed by the gauge symmetry are nonzero. As such the fact that muoquark only couples to muons is imposed by the choice of charge assignments under $U(1)_X$, Eq. (2.12). Similarly, the charge assignments, Eq. (2.13), forbid the proton decay, while quark Yukawas are allowed, Eq. (2.11). In the rest of the section we discuss these requirements in detail.

2.1 General gauged flavor $U(1)_X$

Throughout the manuscript we assume that the SM is extended by three right-handed neutrinos. The chiral fermions of the theory thus carry the following charges under the $SU(3)_C \times SU(2)_L \times U(1)_Y \times U(1)_X$ gauge group,

$$\begin{aligned} Q_i &\sim (\mathbf{3}, \mathbf{2}, \frac{1}{6}, X_{Q_i}), & U_i &\sim (\mathbf{3}, \mathbf{1}, \frac{2}{3}, X_{U_i}), & D_i &\sim (\mathbf{3}, \mathbf{1}, -\frac{1}{3}, X_{D_i}), \\ L_i &\sim (\mathbf{1}, \mathbf{2}, -\frac{1}{2}, X_{L_i}), & E_i &\sim (\mathbf{1}, \mathbf{1}, -1, X_{E_i}), & N_i &\sim (\mathbf{1}, \mathbf{1}, 0, X_{N_i}), \end{aligned} \quad (2.1)$$

with $i = 1, 2, 3$ the flavor index. The $SU(2)_L$ doublets (singlets) are left (right) Weyl spinors under Lorentz symmetry.

A consistent ultraviolet (UV) gauge theory has to be free of chiral anomalies. In this work we require that the $U(1)_X$ charge assignments for the field content in Eq. (2.1) are already anomaly free.¹ This results in six conditions corresponding to the cancellation of (mixed) triangle anomalies between $U(1)_X$, SM gauge groups, and gravity [80],

$$SU(3)_C^2 \times U(1)_X : \sum_{i=1}^3 (2X_{Q_i} - X_{U_i} - X_{D_i}) = 0, \quad (2.2)$$

$$SU(2)_L^2 \times U(1)_X : \sum_{i=1}^3 (3X_{Q_i} + X_{L_i}) = 0, \quad (2.3)$$

$$U(1)_Y^2 \times U(1)_X : \sum_{i=1}^3 (X_{Q_i} + 3X_{L_i} - 8X_{U_i} - 2X_{D_i} - 6X_{E_i}) = 0, \quad (2.4)$$

$$\text{Gravity}^2 \times U(1)_X : \sum_{i=1}^3 (6X_{Q_i} + 2X_{L_i} - 3X_{U_i} - 3X_{D_i} - X_{E_i} - X_{N_i}) = 0, \quad (2.5)$$

$$U(1)_Y \times U(1)_X^2 : \sum_{i=1}^3 (X_{Q_i}^2 - X_{L_i}^2 - 2X_{U_i}^2 + X_{D_i}^2 + X_{E_i}^2) = 0, \quad (2.6)$$

¹Our construction could be viewed as a low-energy effective theory in which anomalies could alternatively be canceled by a higher-dimension Wess-Zumino-Witten operator [78]. The WZW operator is generated by integrating out heavy chiral fermions in the UV. In general, it is not always clear how to make these fermions heavy enough to satisfy the self-consistency of the effective theory assumptions. For an example see, e.g., Ref. [79].

$$U(1)_X^3 : \sum_{i=1}^3 (6X_{Q_i}^3 + 2X_{L_i}^3 - 3X_{U_i}^3 - 3X_{D_i}^3 - X_{E_i}^3 - X_{N_i}^3) = 0 . \quad (2.7)$$

We consider only rational solutions motivated by the unification scenario, i.e., embedding the $U(1)_X$ into a simple Lie group at high-energies. We can work with integer charges without loss of generality, since for any set of rational charges $\{p_{F_i}/q_{F_i}\}$, there is an equivalent set of integer charges obtained by rescaling the gauge coupling g_X with the least common denominator. Any set of integer charges $\{X_{F_i}\}$ satisfying the anomaly conditions (2.2)–(2.7) can be used to generate up to $(3!)^6$ inequivalent solutions (and a correspondingly smaller set, if some of the charges for different families coincide), by permuting the flavor specific charges within each species. Below, we list the solutions to the Diophantine equations (2.2)–(2.7) up to this freedom of family permutations.

Still, this leaves us with infinitely many integer solutions of the anomaly cancellation conditions. For concreteness, we limit the maximal ratio of the largest and the smallest nonzero charge magnitudes to be ≤ 10 .² In the following we then give an exhaustive set of inequivalent integer solutions of Eqs. (2.2)–(2.7) with

$$-10 \leq X_{F_i} \leq 10 \quad \text{for every } F_i \text{ in Eq. (2.1)}, \quad (2.8)$$

building on the work of Ref. [80], while imposing further constraints to produce viable muonquark models.

2.2 Quark flavor universal $U(1)_X$

The symmetry-breaking scalar fields are

$$H = (\mathbf{1}, \mathbf{2}, \frac{1}{2}, X_H) , \quad \phi = (\mathbf{1}, \mathbf{1}, 0, X_\phi) , \quad (2.9)$$

where H is the SM Higgs (with $U(1)_X$ charge X_H) and ϕ is the SM singlet responsible for the breaking of $U(1)_X$. Shifting the $U(1)_X$ charge assignments for all fields by a universal multiple of the hypercharge, $X_F \rightarrow X_F - aY_F$, gives a physically equivalent theory, cf. Appendix A.1. The ambiguity in charge assignments is a direct consequence of the freedom in defining the $U(1)$ subgroups for a symmetry group with several Abelian factors. A familiar example is the QCD, which, ignoring the anomalies, has a global $U(1)_V \times U(1)_A$ or, equivalently, a $U(1)_L \times U(1)_R$ symmetry.

In what follows, we use the above reparameterization invariance to make H a $U(1)_X$ singlet,

$$X_H = 0 , \quad (2.10)$$

and thus H is the usual SM Higgs. To simplify the discussion further, we require all quarks to have the same $U(1)_X$ charge,

$$X_{Q_i} = X_{U_j} = X_{D_k} \equiv X_q , \quad \text{for all } i, j, k = 1, 2, 3, \quad (2.11)$$

such that their masses and the CKM mixing matrix are allowed by the gauge symmetry, i.e. $Y_u^{ij} \bar{Q}^i \tilde{H} u^j$ and $Y_d^{ij} \bar{Q}^i H d^j$ where $\tilde{H} = \epsilon H^*$. The conditions (2.11) reduce the number

²As a point of reference, this ratio is 6 for the SM hypercharge.

of inequivalent sets of X_{F_i} charges in the range $[-10, 10]$ from the original 21 546 920 of Ref. [80] to 276.

The theory will also have a leptoquark field charged under $U(1)_X$ coupled exclusively to muons [1, 76, 77]. To realize the *muoquark* [1], we further impose:

- The leptoquark coupling ($q\ell$ -LQ) is allowed for μ but not for e and τ ,

$$X_{\ell_2} \neq X_{\ell_{1,3}} , \quad (2.12)$$

where ℓ is L or E , i.e., the three flavors of L_i or E_i ($i = 1, 2, 3$) are not all charged the same. Out of 276 sets, 273 satisfy this criteria.

- The diquark couplings (qq -LQ or qqH -LQ) are forbidden and thus proton decay is suppressed, postponing the potential $U(1)_B$ violating effects to dimension-6 operators, the same as in the SM EFT. Given that the color contraction in a diquark (qq -LQ) coupling is $\mathbf{3} \times \mathbf{3} \times \mathbf{3}$ while in the leptoquark coupling ($q\ell$ -LQ) it is $\mathbf{3} \times \bar{\mathbf{3}}$, this implies

$$X_{\ell_2} \neq +3X_q \text{ for } SU(2)_L \text{ doublet scalars, and vectors } \mathbf{1}(\mathbf{3})_{2/3} , \quad (2.13a)$$

$$X_{\ell_2} \neq -3X_q \text{ for } SU(2)_L \text{ singlet and triplet scalars, and vector doublets.} \quad (2.13b)$$

This is satisfied for 272 and 273 sets, respectively.

- The ϕ charge should be chosen such that $qq\phi$ -LQ dimension-5 operators are forbidden, i.e. the $U(1)_B$ stays an accidental symmetry up to dimension-6 Lagrangian.

The observed structure of neutrino masses and mixings may impose further nontrivial constraints on the setup. We make no attempt to impose these constraints when listing the anomaly-free $U(1)_X$ models below, since they depend on whether or not there are additional scalars in the theory. For instance, the $U(1)_{B-3L_\mu}$ model proposed in Ref. [1] requires no additional scalars, since it already admits the minimal realization of the neutrino masses. The nontrivial change from the requirements listed in the bullets above is that now the charge X_ϕ is determined from the structure of the neutrino mass matrix, and in general the proton decay inducing dimension-5 operator $qq\phi$ -LQ could be allowed. This does not happen in the $U(1)_{B-3L_\mu}$ model and no dimension-5 proton decay operator is allowed in the case of a realistic type-I seesaw model that gives the neutrino masses and mixings in agreement with the neutrino oscillations data.

The situation is expected to be different for a generic $U(1)_X$ gauge model. Assuming only the minimal breaking sector will normally impose a texture of the Majorana mass matrix that is too restrictive and will not be able to accommodate the observed neutrino mixing and mass patterns. For example, the minimal type-I seesaw realization of the neutrino mass in $U(1)_{L_\mu-L_\tau}$ introduces dimension-5 proton decay plus shows some tension in fitting θ_{23} and $\sum_i m_{\nu_i}$ [81], calling for additional structure to be added [82]. In general, it is always possible to introduce additional $U(1)_X$ symmetry-breaking scalars whose VEVs then populate the missing entries in the mass matrix. For example, the mass matrix of the right-handed neutrinos can be populated by $\phi_{ij}\bar{N}_i^c N_j$ where $X_{\phi_{ij}} = -X_{N_i} - X_{N_j}$. In such

extensions some care needs to be taken to remove the potential Goldstone bosons, as well as to avoid baryon number violating operators at dimension-5. While the catalog of the models derived in this manuscript provides a good starting point, a detailed discussion of the neutrino sector is beyond the scope of the present work and is left for future studies.

With the above caveat about neutrino masses in mind let us now move to the classification of different anomaly free $U(1)_X$ models. It is remarkable that almost all anomaly-free charge assignments $X_{F_i} \in [-10, 10]$ in the quark flavor universal $U(1)_X$ automatically satisfy the muoquark conditions. The list of charge assignments can be classified into two categories:

$$\textbf{vector category} : X_{L_i} = X_{E_i} \quad \text{for all } i = 1, 2, 3, \quad (2.14)$$

$$\textbf{chiral category} : \text{the rest.} \quad (2.15)$$

In the vector category models the charged lepton Yukawas for all three generations are allowed by the $U(1)_X$ symmetry, while in the chiral category models at least some of the charged lepton Yukawas are forbidden and thus all the lepton masses are generated only after the $U(1)_X$ symmetry is spontaneously broken.

Before discussing each of the two categories in more detail, let us consider several examples of muoquarks adopting the nomenclature from Ref. [75]:

- The scalar leptoquark $S_3 \equiv (\bar{\mathbf{3}}, \mathbf{3}, 1/3, X_{S_3})$, where $X_{S_3} = -X_q - X_{L_2}$, gives $V - A$ contribution to $b \rightarrow s\mu^+\mu^-$ transitions, see e.g. [1, 75, 77, 83–91]. The condition in Eq. (2.13b) implies $X_{L_2} \neq -3X_q$ such that the dimension-4 operator QQS_3 is forbidden.
- The scalar leptoquark $S_1 \equiv (\bar{\mathbf{3}}, \mathbf{1}, 1/3, X_{S_1})$, where $X_{S_1} = -X_q - X_{L_2}$ or $X_{S_1} = -X_q - X_{E_2}$, implemented in “vector category” models, couples to both L_2 and E_2 to give the m_t -enhanced contribution to $(g - 2)_\mu$, see e.g. [1, 75, 87, 91–95]. The condition in Eq. (2.13b) is $X_{L_2} \neq -3X_q$.
- The scalar leptoquark $R_2 \equiv (\mathbf{3}, \mathbf{2}, 7/6, X_{R_2})$, where $X_{R_2} = X_q - X_{L_2}$ or $X_{R_2} = X_q - X_{E_2}$, and the condition in Eq. (2.13a) is $X_{L_2} \neq 3X_q$ such that dimension-5 operator $ddH^\dagger R_2$ is forbidden. Note that otherwise such operators would lead to excessive proton decay even when suppressed by the Planck scale [75, 96, 97]. This scalar leptoquark representation is also used to address the $(g - 2)_\mu$, see e.g. [75, 91, 93, 95]. We will employ it in Section 4 to build a model for radiative muon mass and $(g - 2)_\mu$.
- The vector leptoquark $U_1 \equiv (\mathbf{3}, \mathbf{1}, 2/3, X_{U_1})$, where $X_{U_1} = X_q - X_{L_2}$ or $X_{U_1} = X_q - X_{E_2}$. The baryon number violating dimension-5 operator $QdH^\dagger U_1$ is forbidden when $X_{L_2} \neq 3X_q$, Eq. (2.13a). Possible UV completions for the U_1 vector muoquark will be presented in Section 5. This leptoquark representation was extensively discussed in the literature to address the B -decay anomalies, see e.g. [98–112].

2.2.1 Vector category $U(1)_X$ charge assignments

The vector category is defined such that the left-handed and the right-handed e , μ and τ leptons carry the same X charge. Solutions to the anomaly conditions (2.2)–(2.7) that

further satisfy Eqs. (2.11) and (2.14) are parameterized by [61]

$$X_F = X_e T_{L_e} + X_\mu T_{L_\mu} + X_\tau T_{L_\tau} - \left(\frac{X_e + X_\mu + X_\tau}{3} \right) T_B + a Y_F + \sum_i X_{N_i} T_{N_i}, \quad (2.16)$$

where $\{T_B, T_{L_e}, T_{L_\mu}, T_{L_\tau}\}$ are the usual baryon and lepton numbers for the SM fermions, while T_{N_i} are the right-handed neutrino numbers (also $T_{B, L_{e, \mu, \tau}} N_i = 0$). The reparameterization, $X_F \rightarrow X_F - a Y_F$, allows to restrict the discussion to the case $a = 0$. The coefficients $\{X_e, X_\mu, X_\tau, X_{N_1}, X_{N_2}, X_{N_3}\}$ in Eq. (2.16) need to satisfy the Diophantine equations [80, 113]

$$X_e + X_\mu + X_\tau = \sum_i X_{N_i}, \quad X_e^3 + X_\mu^3 + X_\tau^3 = \sum_i X_{N_i}^3. \quad (2.17)$$

We group the solutions to the above equations in three non-exclusive classes, up to arbitrary permutations in flavor indices $\{e, \mu, \tau\}$ and $\{N_1, N_2, N_3\}$,

$$\text{Class 1 : } \quad X_e = X_{N_1}, \quad X_\mu = X_{N_2}, \quad X_\tau = X_{N_3}, \quad (2.18)$$

$$\text{Class 2 : } \quad X_e = X_{N_1}, \quad X_\mu = -X_\tau, \quad X_{N_2} = -X_{N_3}, \quad (2.19)$$

$$\text{Class 3 : } \quad \text{the rest.} \quad (2.20)$$

This generalizes the results from Ref. [61], where only the Class 1 solutions were considered. The Class 1 and Class 2 solutions are three-parameter family of solutions, with $\{X_e, X_\mu, X_\tau\}$ and $\{X_e, X_\mu, X_{N_2}\}$ taken as free parameters in Eqs. (2.18) and (2.19), respectively. The solutions that have $X_\mu = X_{N_2} = -X_\tau = -X_{N_3}$ are both of Class 1 and Class 2.

Scanning over the general results from Ref. [80] (see also [114]) for the anomaly-free $U(1)_X$ extensions of the SM, we find the charge assignments that satisfy the anomaly conditions (2.2)–(2.7), the charged lepton condition (2.14), the muoquark conditions (2.12)–(2.13), and have the ratio between the largest and the smallest nonzero charge magnitudes 10 or less. There are in total 252 for Eq. (2.13b) and 251 for Eq. (2.13a). Out of these 77 (or 76) belong to Class 1, 185 to Class 2 (with 12 both in Class 1 and Class 2), while there are two exceptional (Class 3) charge assignments. These are (up to flavor permutations),

$$\{X_e, X_\mu, X_\tau\} = \{-5, -1, 6\}, \quad \{X_{N_1}, X_{N_2}, X_{N_3}\} = \{-3, -2, 5\}, \quad \text{and} \quad (2.21)$$

$$\{X_e, X_\mu, X_\tau\} = \{-3, -2, 5\}, \quad \{X_{N_1}, X_{N_2}, X_{N_3}\} = \{-5, -1, 6\}. \quad (2.22)$$

Class 1 and 2 models can be considered to be vector-like solutions to the Diophantine Eq. (2.17), in the usual physics nomenclature from anomaly cancellations. Indeed, any numbers satisfying Eqs. (2.18)–(2.19) automatically satisfy the Diophantine equations (2.2)–(2.7). Upon relaxing our search requirement $|X_{F_i}| \leq 10$, all solutions of Class 1 and 2 are parameterized by three arbitrary integers (X_e, X_μ, X_τ) and (X_e, X_μ, X_{N_2}) , respectively. Class 3 models, corresponding to chiral solutions of the Diophantine equation, are not easily parameterized beyond $|X_{F_i}| \leq 10$. However, given some effort this problem has been solved [114].

X_{L_1}	X_{L_2}	X_{L_3}	b_{E_1}	X_{N_1}	X_{N_2}	X_{N_3}
-1	-1	2	-1	-2	-1	3
-6	-1	7	-1	-7	-2	9
-5	-2	7	-2	-7	-3	10
-3	-2	5	-2	-9	-1	10
-5	-1	6	-1	-9	-1	10
-2	5	6	2	1	3	5
-1	5	5	2	1	3	5
-3	5	7	2	1	3	5
0	4	5	1	1	3	5
2	2	5	-1	1	3	5
-4	5	8	2	1	3	5
-3	4	8	1	-1	3	7
-2	4	7	1	-1	4	6
-3	6	6	3	3	3	3
1	1	7	-2	-3	5	7
-2	2	9	-1	-6	5	10
-1	2	8	-1	-6	7	8
3	5	10	-1	2	6	10

Table 1. Charge assignments (up to family permutations) for $b_{E_1} = -b_{E_2}/2 = b_{E_3}$ case (Category II) with maximal ratio of nonzero charges less or equal to 10. See Section 2.2.2 for details.

2.2.2 Chiral category $U(1)_X$ charge assignments

There are additional 21 charge assignments for $X_{F_i} \in [-10, 10]$ for which the right-handed e , μ and τ charges changes to

$$X_{E_1} = X_{L_1} + b_{E_1}, \quad (2.23)$$

$$X_{E_2} = X_{L_2} + b_{E_2}, \quad (2.24)$$

$$X_{E_3} = X_{L_3} + b_{E_3}. \quad (2.25)$$

while the other charges are still given by the parameterization in Eq. (2.16). The 18 solutions that have

$$b_{E_1} = -b_{E_2}/2 = b_{E_3}, \quad (2.26)$$

are listed in Table 1 (up to flavor permutations). The remaining three solutions are

$$\{X_{L_{1,2,3}}\} = \{-7, 0, 7\}, \quad \{b_{E_{1,2,3}}\} = \{-1, 3, -2\}, \quad \{X_{N_{1,2,3}}\} = \{-5, -3, 8\}, \quad (2.27)$$

$$\{X_{L_{1,2,3}}\} = \{-5, -3, 8\}, \quad \{b_{E_{1,2,3}}\} = \{-2, 3, -1\}, \quad \{X_{N_{1,2,3}}\} = \{-6, -4, 10\}, \quad (2.28)$$

$$\{X_{L_{1,2,3}}\} = \{-5, 6, 8\}, \quad \{b_{E_{1,2,3}}\} = \{1, -3, 2\}, \quad \{X_{N_{1,2,3}}\} = \{0, 3, 6\}. \quad (2.29)$$

These solutions are particularly interesting as they facilitate models in which the muon mass and the $(g-2)_\mu$ are both generated at one-loop order (see Section 4).

3 Light X_μ phenomenology

When the $U(1)_X$ gauge boson X_μ is light, it can give the dominant new physics contribution to $(g-2)_\mu$ and potentially resolve the discrepancy between the measurements and the SM prediction, see e.g. [115]. In this section we show that the $(g-2)_\mu$ anomaly can indeed be explained, without violating other experimental constraints, by a sub-GeV vector boson X_μ in a broad class of $U(1)_X$ gauge models. The $U(1)_X$ models that we consider all admit the muon solution of the rare B decay anomalies in the $R_{K^{(*)}}$ ratios and $b \rightarrow s\mu\mu$ angular distributions and branching ratios.

The model independent discussion in Sections 3.1, 3.2, and 3.3 is limited to the flavor conserving X_μ couplings applicable for the $U(1)_X$ gauge models. Section 3.4 contains also a short discussion of challenges facing a light vector boson that would be flavor violating [116]. The main goal of Section 3.4 is to show that a single light X_μ cannot simultaneously resolve both the $(g-2)_\mu$ and rare B decay anomalies, and therefore another heavy mediator such as $S_3 \equiv (\bar{\mathbf{3}}, \mathbf{3}, 1/3, X_{S_3})$ is required. Section 3.5 then contains several benchmark models that can solve both the $(g-2)_\mu$ and rare B decay anomalies, with most of the phenomenological discussion focused on X_μ while for the S_3 phenomenology we refer to [1, 77, 84, 87, 88].

3.1 Muon $(g-2)_\mu$

Recently, the Muon $g-2$ collaboration at the Fermilab announced its first preliminary measurement of the muon anomalous magnetic moment [117–119], consistent with the BNL result [2]. The combination of the two experimental results (a_μ^{avg}) differs by 4.2σ [117] from the SM prediction (a_μ^{SM}),³

$$\Delta a_\mu^R = a_\mu^{\text{avg}} - a_\mu^{\text{SM}} = (251 \pm 59) \times 10^{-11}. \quad (3.1)$$

The SM prediction obtained on the lattice by the BMW collaboration [25], on the other hand, differs by only 1.6σ from the experimental average, and is thus consistent with $\Delta a_\mu = 0$. In the numerical studies we use Eq. (3.1) with the caveat that the situation calls for further studies of the SM prediction.

The light gauge boson X_μ that couples to muons,

$$\mathcal{L} \supset g_X \bar{\mu} \not{X} (q_V - q_A \gamma_5) \mu, \quad (3.2)$$

gives the following 1-loop contribution to the muon anomalous magnetic moment, see, e.g., Refs. [115, 122],

$$\Delta a_\mu = \frac{g_X^2}{8\pi^2} r_\mu^2 [q_V^2 I_V(r_\mu) + q_A^2 I_A(r_\mu)] = \frac{g_X^2}{8\pi^2} \begin{cases} q_V^2 - 2r_\mu^2 q_A^2, & m_X \ll m_\mu \\ \frac{2}{3} r_\mu^2 [q_V^2 - 5q_A^2], & m_X \gg m_\mu \end{cases}, \quad (3.3)$$

where $r_\ell = m_\ell/m_X$ and

$$I_V(r_\ell) = \int_0^1 dx \frac{2x^2(1-x)}{1-x+r_\ell^2 x^2}, \quad I_A(r_\ell) = - \int_0^1 dx \frac{2x(1-x)(4-x) + 4r_\ell^2 x^3}{1-x+r_\ell^2 x^2} \quad (3.4)$$

³Obtained from the measurements of R -ratios, see [3] and reference therein. This prediction is supported by the electroweak precision tests, where the same $e^+e^- \rightarrow \text{hadrons}$ data is used to calculate $\alpha(m_Z)$ [120, 121].

Both $I_V(r_\ell)$ and $I_A(r_\ell)$ are monotonic functions of m_X such that the vector (axial) contributions to a_μ are always positive (negative). Thus, in order to account for the central value of Δa_μ in Eq. (3.1), the vector coupling needs to be nonzero, $q_V \neq 0$. Numerically,

$$g_X = \left(\frac{\Delta a_\mu}{251 \times 10^{-11}} \right)^{1/2} \begin{cases} 4.5 \times 10^{-4} [q_V^2 - 2q_A^2 r_\mu^2]^{-1/2}, & m_X \ll m_\mu, \\ 5.5 \times 10^{-4} r_\mu^{-1/2} [q_V^2 - 5q_A^2]^{-1/2}, & m_X \gg m_\mu. \end{cases} \quad (3.5)$$

For m_X below or comparable with the muon mass, the gauge coupling required to explain the observed Δa_μ is $g_X \sim \mathcal{O}(10^{-4})$. To get the correct sign, Eq. (3.5) implies that X_μ needs to predominantly couple vectorially, with the axial-to-vector ratio of couplings required to be below $|q_A/q_V| < m_X/(\sqrt{2}m_\mu) \ll 1$ when $m_X \ll m_\mu$, and below $|q_A/q_V| < 1/\sqrt{5}$ when $m_\mu \ll m_X$.

3.2 Neutrino trident production

The neutrino trident production provides important bounds on the muonic force explanations of the $(g-2)_\mu$ anomaly. The muon neutrino and the left-handed muon form an electroweak doublet and thus share the same coupling to X_μ , proportional to $\propto (q_V + q_A)$. Since any explanation of the $(g-2)_\mu$ anomaly must be mostly vectorial, a flavor diagonal explanation of the $(g-2)_\mu$ anomaly necessarily implies NP contributions to the trident production $\nu_\mu N \rightarrow \nu_\mu N \mu^+ \mu^-$ induced by the ν_μ neutrino scattering on nucleus N . The strongest bound on the NP contributions to the trident production cross section is from the CCFR experiment that reported $\sigma_{\text{CCFR}}/\sigma_{\text{SM}} = 0.82 \pm 0.28$ [123], where σ_{CCFR} is the measured cross section and σ_{SM} the SM prediction.

The calculation of the trident production cross section in the presence of NP was performed in Ref. [48], by considering the scattering of neutrinos on the potential photons sourced by the nucleus, $\nu_\mu \gamma \rightarrow \nu_\mu \gamma \mu^+ \mu^-$. The corresponding matrix element squared is given by

$$|\mathcal{M}_{\nu_\mu \gamma}|^2 = |\mathcal{M}_0|^2 \left(\left[C_V^{\text{SM}} - C_V^X \frac{m_X^2}{k^2 - m_X^2} \right]^2 + \left[C_A^{\text{SM}} - C_A^X \frac{m_X^2}{k^2 - m_X^2} \right]^2 \right), \quad (3.6)$$

where k is the momentum flowing through the X_μ propagator in the NP tree level diagram. The SM contribution is due to the W/Z exchanges and is encoded in the coefficients $C_V^{\text{SM}} = \frac{1}{2} + 2 \sin^2 \theta_W$ and $C_A^{\text{SM}} = \frac{1}{2}$, and in the common prefactor \mathcal{M}_0 . The NP contributions are given by the NP coefficients

$$C_{V,A}^X = g_X^2 q_{V,A} (q_V + q_A) \frac{v_{\text{SM}}^2}{m_X^2}, \quad (3.7)$$

conveniently normalized to the Fermi constant.

In the numerical results we use the recast of experimental results from Ref. [48], but with an appropriate approximation that extends it to the case of nonzero, yet still subleading, axial couplings of X_μ . In Ref. [48] the integrated cross section $\sigma(\nu_\mu N \rightarrow \nu_\mu N \mu^+ \mu^-)$ was computed for a purely vectorial NP force with $q_A = 0$, $q_V = 1$, and the bounds on the couplings were deduced by comparing the predictions with the experimental measurements,

paying special attention to the experimental cuts. In Eq. (3.6), because $C_V^{\text{SM}} \neq C_A^{\text{SM}}$, the NP axial coupling has a different relative weight between the pure NP contribution and the interference term with the SM. Consequently, the phenomenological analysis of Ref. [48] does not apply without changes to the more general case of Eq. (3.6). In Appendix B.1 we explain in detail how to reinterpret this bound with $\mathcal{O}(10\%)$ accuracy.

3.3 Other constraints

Borexino

The Borexino experiment measured a cross section for the elastic scattering of ${}^7\text{Be}$ solar neutrinos on electrons [124, 125]. Because of neutrino oscillations the flux on Earth is composed of all three neutrino flavors incoherently scattering on electrons. The tree-level X_μ exchanges can modify the scattering rate from the SM expectation. Since no deviation was observed, this implies bounds on X_μ couplings to fermions that are due to a combination of direct $U(1)_X$ charges and induced couplings from kinetic mixing of X_μ with the photon (in particular to the electron). For the numerical estimates we closely follow the analysis in Ref. [49]. The bound becomes stronger if X_μ also couples to tau and electron neutrinos in addition to the muon neutrino and becomes weaker if the direct coupling of X_μ to the electron cancels against the kinetic-mixing-induced one.

Light resonance searches

New light resonances can be probed by a number of intensity frontier experiments, summarized, e.g., in Refs. [126, 127]. In the numerical estimates we mostly use DARKCAST [126] to recast the existing and future projections of dark photon bounds. The $X\mu\mu$ coupling is currently probed by NA62 ($K \rightarrow \mu\nu X$ decays) [128, 129], and BaBar (searches for $X \rightarrow \mu\mu$ decays in the 4μ final state) [130]. In case of couplings to baryon number and/or to electron via kinetic mixing there are additional bounds from the LHCb dark photon searches [131–133], NA64 [134], BaBar [135] and NA62 (invisible π^0 decays) [136].

For future projections on the sensitivity to $X\mu\mu$ coupling we consider NA64 $_\mu$ [137–140], M³ [141], Belle-II [142], NA62 [128] and ATLAS [143]. For other couplings (e.g. to hadrons) we also consider the projections for LHCb from Ref. [131].

Astrophysics and Cosmology

The parameter region of interest easily passes the astrophysical and cosmological constraints. The X_μ decays to neutrinos before the onset of BBN for $m_X \gtrsim 6$ MeV [144]. The potential supernova 1987A limits discussed in [145] (see [146] for the robustness of the bound) apply to much smaller couplings in the considered mass range. That is, the values of g_X relevant for the explanation of the $(g-2)_\mu$ anomaly lead to X_μ trapping in the proto-neutron star and, therefore, to no cooling constraints.

3.4 A single mediator for both $(g-2)_\mu$ and rare B decay anomalies?

An interesting question is whether a single mediator could be responsible for both the $(g-2)_\mu$ and rare B decay anomalies. Here we explore to what extent this is possible when

the mediator is a neutral spin-1 boson, X_μ . We keep the discussion quite general so that the results also apply to the different $U(1)_X$ models.

We construct an EFT with the dynamical gauge field X_μ and the $U(1)_X$ symmetry-breaking scalar ϕ , while the rest of the BSM spectrum is integrated out. In particular, the quark flavor-violating Xbs interaction, needed to explain the anomalies in rare B decays, is a result of some unspecified short-distance physics (e.g., from integrating out heavy vector-like fermions). The relevant effective X_μ interactions are given by

$$\begin{aligned} \mathcal{L}_{\text{eff}} \supset &+ g_X (q_V + q_A) \bar{\nu}_{\mu L} \not{X} \nu_{\mu L} + g_X \bar{\mu} \not{X} (q_V - q_A \gamma_5) \mu \\ &+ \left[\bar{b} \not{X} (g_L^{bs} P_L + g_R^{bs} P_R) s + \text{H.c.} \right], \end{aligned} \quad (3.8)$$

extending the effective Lagrangian in Eq. (3.2). For $U(1)_X$ models, the second line can arise from higher-dimension gauge invariant operators, for example from $(\phi^\dagger D_\mu \phi)(\bar{Q}_2 \gamma^\mu Q_3), \dots$, after the breaking of $U(1)_X$ by the ϕ VEV. The flavor-diagonal couplings to muons and muon neutrinos, on the other hand, occur in $U(1)_X$ models directly from charging them under the $U(1)_X$ group.

The EFT in Eq. (3.8) allows us to address the following question: Can the anomalies in both $(g-2)_\mu$ and rare B decays be explained by one-loop and tree-level exchanges of X_μ , respectively, or is an additional short-distance contribution needed?

The NP effects that could explain $R_{K^{(*)}}$ and the $b \rightarrow s\mu\mu$ anomalies can be expressed in terms of the modified Wilson coefficients C_9 and C_{10} that we define as in Ref. [38]. The tree-level X_μ exchanges contribute as (cf. [147])

$$C_{9,10}^{(\prime)} = \frac{q_{V,A}}{N} \frac{g_X g_{L(R)}^{bs}}{q^2 - m_X^2 + im_X \Gamma_X}, \quad (3.9)$$

where $N = \frac{G_F \alpha}{\sqrt{2} \pi} V_{tb} V_{ts}^*$ is a normalization factor. The Xbs couplings $g_{L(R)}^{bs}$ are stringently constrained, e.g. by $\text{BR}(B \rightarrow K\nu\nu)$ if X_μ is lighter than the B meson or by the B_s neutral meson mixing. Since right-handed quark couplings are not needed to explain the anomalies in rare B decays (cf. e.g. [38]), in the following we set $g_R^{bs} = 0$. Here we focus on light X_μ with $m_X < m_B - m_K$, such that the most important constraint on g_L^{bs} comes from $\text{BR}(B \rightarrow K\nu\nu)$ [148–151]. For $\text{BR}(X \rightarrow \nu\nu) \simeq 1$, this bound is given by [147]

$$g_L^{bs} \lesssim 0.7 \times 10^{-8} \frac{m_X}{\text{GeV}}. \quad (3.10)$$

Consequently, an explanation of $R_{K^{(*)}}$ and the $b \rightarrow s\mu\mu$ anomalies requires sizable $X\mu\mu$ couplings.

Let us now consider the one-loop contributions to $(g-2)_\mu$ from X_μ and either e , μ or τ running in the loop (and forget for the moment about the UV completions). For e and τ running in the loop, the X_μ couplings are flavor violating, a possibility suggested in [116]. The $(g-2)_\mu$ excess can in principle be explained by the flavor violating $X\mu\tau$ coupling, with $m_X > 1.7 \text{ GeV}$. In contrast, the $Xe\mu$ coupling leads to a negative contributions to Δa_μ . For the flavor conserving option, with X_μ coupling to muons inducing the $(g-2)_\mu$ at one loop, is viable, as long as vector couplings are larger than axial ones, see the discussion

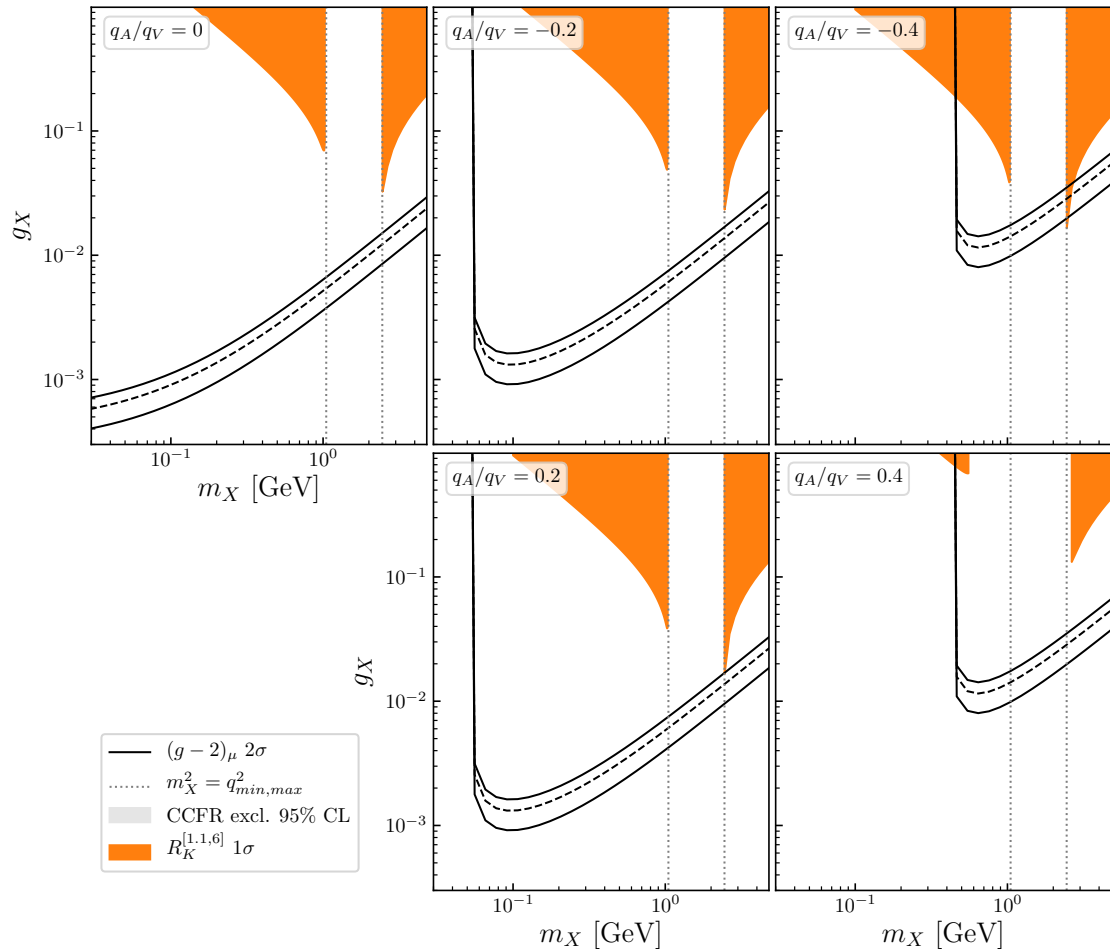


Figure 1. Parameter space for the light X_μ solution to the $(g-2)_\mu$ anomaly with the 2σ region and the central values in solid and dashed black, respectively. The gray region is excluded by the neutrino trident production (see Section 3.4). In the orange region, the LHCb measurement of $R_K^{[1.1,6]}$ can be explained at the 1σ level while satisfying the constraint on $q_{L,R}^{bs}$ from $\text{BR}(B \rightarrow K\nu\nu)$.

in Section 3.1. If we want to explain $(g-2)_\mu$ and the anomalies in rare B decays at the same time, the requirement of a sizable $X\mu\mu$ coupling to explain the latter precludes an explanation of $(g-2)_\mu$ predominantly through flavor violating $X\mu\tau$ couplings. The presence of both $X\mu\tau$ and $X\mu\mu$ couplings would lead to too large $\text{BR}(\tau \rightarrow 3\mu)$ in conflict with experimental bounds [152]. This leaves us with the possibility that both the $(g-2)_\mu$ and rare B decay anomalies could be due to flavor diagonal $X\mu\mu$ couplings.

In Fig. 1 we show the regions in the $m_X - g_X$ plane, in which a light X_μ with couplings given by Eq. (3.8) can explain the measured values of $(g-2)_\mu$ and R_K for different choices of q_A/q_V .⁴ The region where the $(g-2)_\mu$ measurement can be explained at the 2σ

⁴In Fig. 1 the Xee couplings were set to zero. However, even if these were allowed to vary, the conclusions would not have changed. The $X\mu\mu$ coupling, needed to explain the $(g-2)_\mu$ anomaly, is expected to be much

level is represented by solid black lines (dashed black lines give the central values). The viable region becomes smaller and moves to larger values of g_X as $|q_A/q_V|$ increases. For $|q_A/q_V| > 1/\sqrt{5} \approx 0.45$, no explanation is possible anymore (cf. Section 3.1). The orange shaded area shows the m_X and g_X values that can explain the LHCb measurement of R_K [34] at the 1σ level, while g_L^{bs} satisfies Eq. (3.10). Since R_K is measured in a bin of the invariant dilepton mass squared, $q^2 \in [1.1, 6] \text{ GeV}^2$, an X_μ with $m_X^2 \in [1.1, 6] \text{ GeV}^2$ can only enhance R_K if it couples to muons (this is further discussed in Appendix B.3). The boundaries of this region are shown in Fig. 1, as gray dotted lines. In conclusion, the measured value of R_K cannot be explained for $m_X^2 \in [1.1, 6] \text{ GeV}^2$. Outside this mass window, as expected from fits to R_K in the $C_9^\mu - C_{10}^\mu$ plane (see e.g. [38]), we find that R_K can be explained for vanishing and negative q_A/q_V and that sizable positive q_A/q_V can preclude an explanation.

The most important constraint on the parameter space shown in Fig. 1 is due to neutrino trident production (cf. Section 3.2). The gray shaded area is excluded at 95% C.L. by the CCFR measurement. When this constraint is satisfied, it is only possible to explain $(g-2)_\mu$ for $|q_A/q_V| \lesssim 0.2$ and $m_X \lesssim 400 \text{ MeV}$. An explanation of R_K for $m_X < m_B - m_K$ is even completely excluded by the CCFR bound.⁵ This, in particular, applies to the small window at $m_X \simeq 2.5 \text{ GeV}$ and $q_A/q_V \simeq -0.4$, where a combined explanation of $(g-2)_\mu$ and R_K would be possible otherwise [147]. We conclude that a single mediator m_X cannot explain both the $(g-2)_\mu$ and rare B decay anomalies while satisfying all constraints as long as the couplings of left-handed muon and muon neutrino are related by $SU(2)_L$ gauge invariance.

3.5 Benchmarks

For the benchmarks we focus on the extended gauge sector from gauging the $U(1)_X$ groups discussed in Section 2. After EWSB, the relevant part of the Lagrangian reads

$$\mathcal{L} \supset -\frac{1}{4}F_{\mu\nu}^2 - \frac{1}{4}X_{\mu\nu}^2 + \frac{1}{2}\varepsilon F_{\mu\nu}X^{\mu\nu} + \frac{1}{2}m_X^2 X_\mu^2 + eA_\mu J_{\text{EM}}^\mu + g_X X_\mu J_X^\mu, \quad (3.11)$$

where $J_{\text{EM},X}^\mu$ are the EM current and the current associated with $U(1)_X$, respectively. This ignores a small $X_\mu - Z_\mu$ mixing proportional to the kinetic-mixing parameter ε , which we will assume to be no larger than $\mathcal{O}(g_X)$. We relegate further details about the mixing of EW and X_μ gauge bosons to Appendix A.2.

The X_μ couplings to the SM fermions are determined by the form of the current J_X^μ and by the size of kinetic mixing parameter ε . The J_X^μ is determined by the $U(1)_X$ SM fermion charges X_f ,

$$J_X^\mu = \sum_f X_f \bar{f} \gamma^\mu f, \quad (3.12)$$

and is specific to each model we consider. The value of ε we treat as a free parameter, with the exception of the $L_\mu - L_\tau$ model, where we follow the literature and assume that the kinetic mixing is generated exclusively by the mass difference between the tau and the muon

larger than the size of Xee coupling allowed by the bounds from the light resonance searches, cf. Section 3.3.

⁵Since the stringent bound on g_L^{bs} from $\text{BR}(B \rightarrow K\nu\nu)$ does not apply for $m_X > m_B - m_K$, it is possible to explain R_K in this higher mass region.

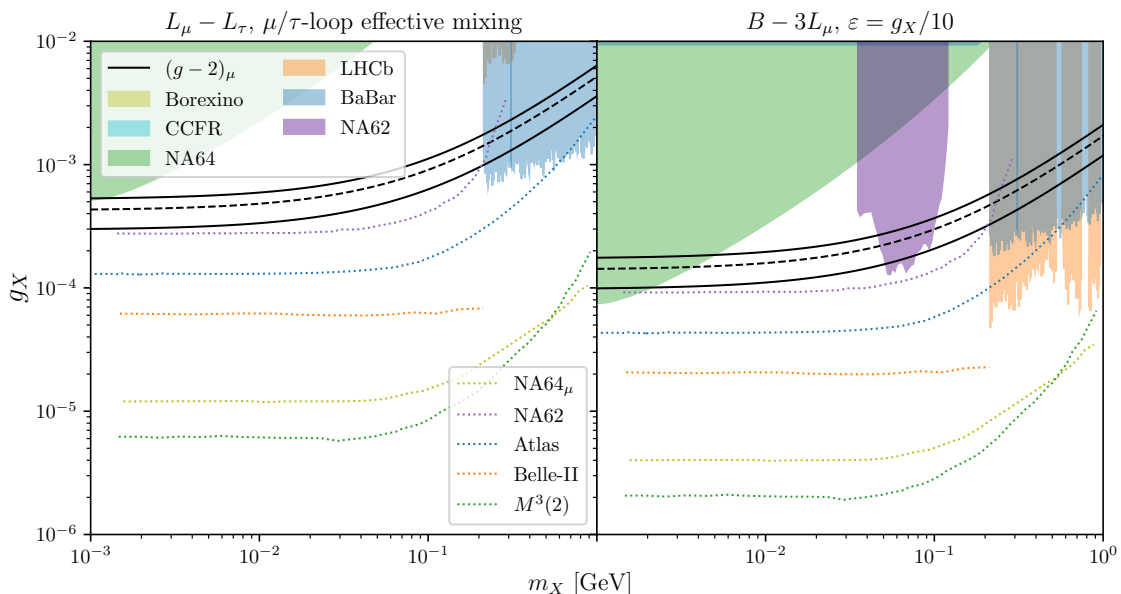


Figure 2. Parameter space for the light X_μ solution of the $(g-2)_\mu$ anomaly in the $U(1)_{L_\mu-L_\tau}$ model (left) and $B-3L_\mu$ model (right). The shaded regions are excluded by various experiments, as denoted in the legend, with dotted lines giving the future projections for the exclusions, while the 2σ region between the black solid lines is preferred by $(g-2)_\mu$ (dashed line for central values).

running in the loop, and is therefore completely predicted with the size $\varepsilon \sim \mathcal{O}(eg_X/16\pi^2)$, see Section 3.5.2 for details. This relies on the assumption that ε vanishes at the high scale (as required in gauge coupling unification). Furthermore, for $U(1)_{L_\mu-L_\tau}$ the kinetic mixing parameter ε has vanishing β function above the EW scale at 1-loop, while the 2-loop contribution is $(m_\tau^2 - m_\mu^2)/v^2$ suppressed. It is thus appropriate to make the approximation in the $U(1)_{L_\mu-L_\tau}$ model that the kinetic mixing only receives the contributions from muons and taus. The other benchmark models we consider have a nonzero β -function for the kinetic mixing parameter ε . Thus, for these model we do not expect $\varepsilon = 0$ except for special tuning points. Typically, it is reasonable to assume $\varepsilon \lesssim g_X$, which is what we use in the sample plots. The 1-loop running of the ε parameter is further analyzed in Appendix A.3.

All the models allow for the S_3 muoquark to be part of the spectrum. We assume that this is the case, which means that both $(g-2)_\mu$ and the anomalies in rare B decays can be explained simultaneously. In the rest of this section we focus on the part of the phenomenology that is relevant for explaining the $(g-2)_\mu$ anomaly, i.e., on the constraints on the couplings of the light gauge boson, X_μ .

3.5.1 Gauged $L_\mu - L_\tau$

For completeness we start the list of benchmark models with the $L_\mu - L_\tau$ gauge symmetry, which has a long history as an explanation for the $(g-2)_\mu$ anomaly [45, 46, 48]. The SM 2nd and 3rd generation leptons are charged oppositely, and thus form vector-like representations

under $U(1)_{L_\mu-L_\tau}$:

$$X_e = X_{N_1} = 0, \quad X_\mu = -X_\tau = 1, \quad X_{N_2} = -X_{N_3}. \quad (3.13)$$

Note that the right-handed neutrinos can carry vector-like charges that are independent of the charges of the SM leptons. However, as long as these are not excessively large (or if the right-handed neutrinos are heavy) we do not expect them to significantly change the phenomenology.

In Fig. 2 (left) we show with black lines the 1σ parameter band (dashed black for central values), where the $L_\mu - L_\tau$ model can account for the observed $(g-2)_\mu$. The model is not expected to have any appreciable kinetic mixing parameter and thus the UV value of ε is set to zero. At one loop the muon and tau kinetic mixing diagrams nevertheless contribute an effective momentum-dependent mixing already accounted for in the DARKCAST model [49, 153], which gives an effective coupling of X_μ to the electrons at the percent level. The resulting constraints (future projections) in Fig. 2 (left) are thus taken directly from DARKCAST and are shown as shaded colored regions (dashed lines) with color coding denoted in the two legends.

3.5.2 Gauged $B - 3L_\mu$

The $B - 3L_\mu$ gauge group has charges

$$X_\mu = X_{N_2} = -3, \quad X_{e,\tau} = X_{N_1,N_2} = 0, \quad X_{Q_i,U_i,D_i} = \frac{1}{3}. \quad (3.14)$$

This is another example of the vector category $U(1)_X$ charge assignments. The $U(1)_{B-3L_\mu}$ was the first gauge group used in a muoquark construction [1]. This group is particularly suitable for the task at hand because it allows for a phenomenologically viable type-I seesaw with only one symmetry-breaking scalar while still forbidding $U(1)_B$ -violating dimension-5 operators. In contrast to the $L_\mu - L_\tau$ model, a sizable kinetic mixing parameter is generated by the RG running. As a reasonable choice, we take as benchmark numerical value $\varepsilon = 0.1g_X$.

The bounds on the $B - 3L_\mu$ model in the sub-GeV mass region for the light vector, which can explain the $(g-2)_\mu$ anomaly (black lines), is reported in Fig. 2 (right). The new features, with respect to the plot on the left, are the NA62 and LHCb bounds due to the quark couplings. The bound from Borexino (red region), mainly sensitive to the electron coupling, allows for a possible solution to the $(g-2)_\mu$ anomaly when $m_X \gtrsim 10$ MeV, while the BaBar bound kicks in at $m_X \geq 2m_\mu$. This leaves an unconstrained region $200 \text{ MeV} \gtrsim m_X \gtrsim 10 \text{ MeV}$ and $g_X \sim 2 \times 10^{-4}$ that can explain the $(g-2)_\mu$ anomaly.

3.5.3 Gauged $L_e - L_\mu$

As an alternative to the $L_\mu - L_\tau$ model, a simple permutation of the charges gives a model with the gauged $L_e - L_\mu$ symmetry,

$$X_\tau = X_{N_3} = 0, \quad X_\mu = -X_e = 1, \quad X_{N_2} = -X_{N_1}. \quad (3.15)$$

The large electron charge greatly enhances the X_μ interactions with electrons. Since such couplings are targeted by many of the light-sector searches one may naively expect for the experimental searches to disqualify the $U(1)_{L_e-L_\mu}$ model as an explanation of $(g-2)_\mu$.

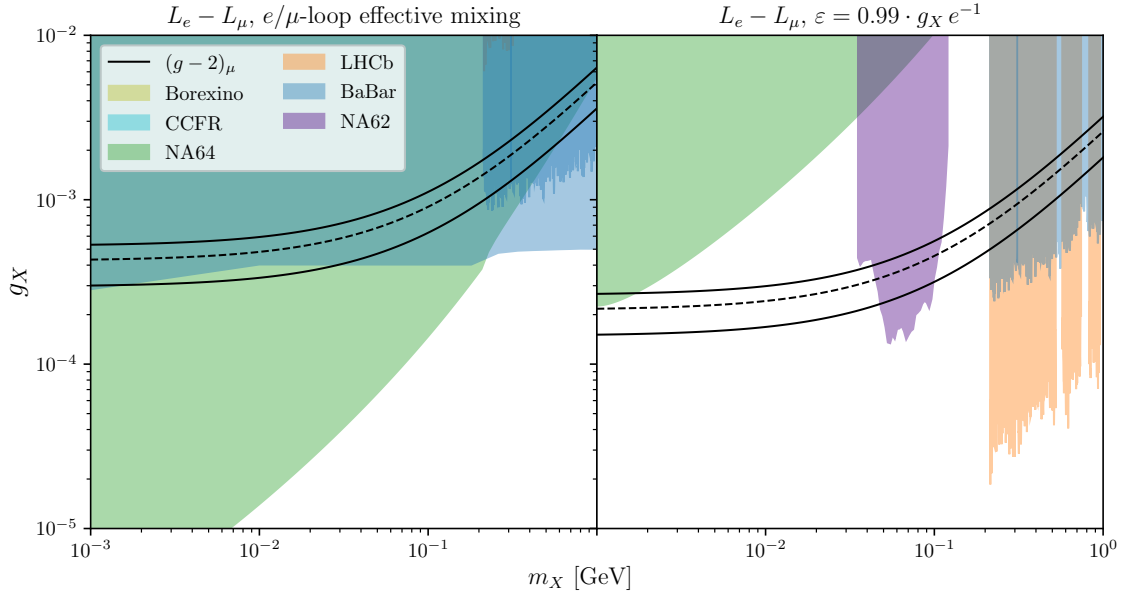


Figure 3. Parameter space for the light X solution to the $(g-2)_\mu$ anomaly in the $U(1)_{L_e-L_\mu}$ model. The shaded regions are excluded by various experiments, as denoted in the legend, while the 2σ region between the black lines is preferred by $(g-2)_\mu$ (dashed lines denote central values).

While this expectation is indeed borne out in most of the parameter space, a loophole that circumvents the stringent electron based bounds is if the kinetic mixing cancels part of the coupling of the physical X_μ to the electrons. The effective charge of the electron is given by

$$X_{\text{eff}} = X_e - \frac{e}{g_X} \varepsilon, \quad (3.16)$$

so it is possible that $|q_{\text{eff}}| \ll 1$ for a suitable choice of ε . Fig. 3 (left) gives the constraints that are obtained for $\varepsilon = 0$ in the UV, in which case the $(g-2)_\mu$ preferred region is excluded (2σ band between the black solid lines, dashed line denotes the central values). Fig. 3 (right), on the other hand, illustrates that a window of parameter space opens up, in which $(g-2)_\mu$ explanation is still phenomenologically viable, if there is a % -level tuning between direct couplings to the electrons and the one induced by kinetic mixing parameter ε . Equivalently, this can be viewed as adjusting the charges with a hypercharge-proportional component in such a manner as to leave the electron uncharged (see Appendix A.1). Indeed the plot on the right is similar to Fig. 2 (right).

3.5.4 Chiral models

We now entertain some of the more exotic options for the $U(1)_X$ group from among the models of Sec. 2.2.2 with chiral charge assignments.

$\tilde{L} - 3B$ model:

$$(X_{L_1}, X_{L_2}, X_{L_3}) = (-3, 8, 4), \quad (X_{E_1}, X_{E_2}, X_{E_3}) = (-2, 9, 2),$$

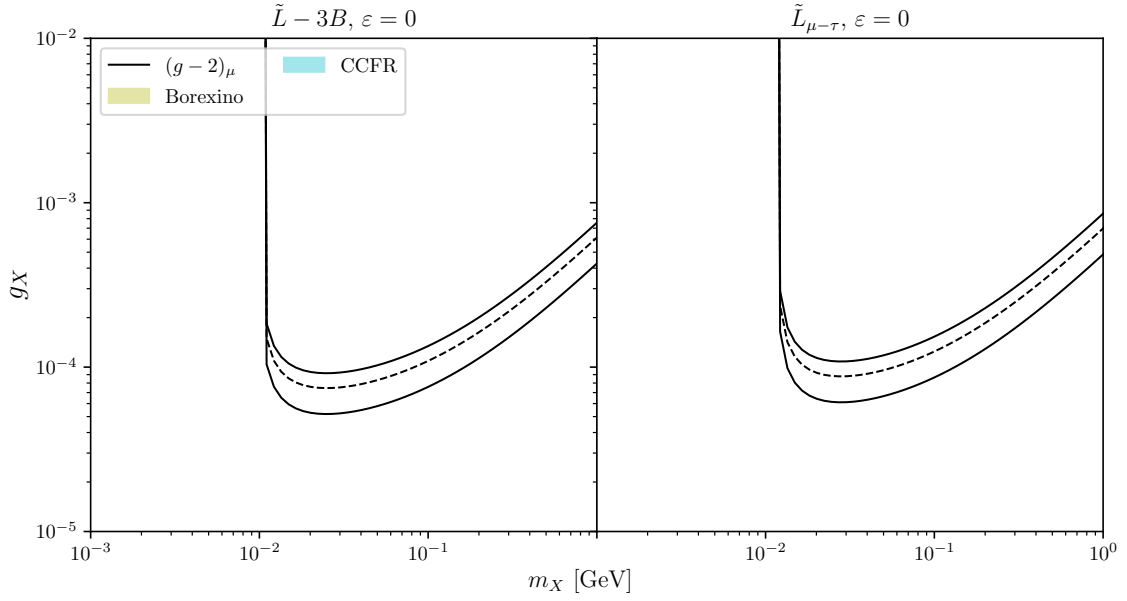


Figure 4. Parameter space for the light X solution to the $(g-2)_\mu$ anomaly in the $U(1)_{\tilde{L}-3B}$ model. The shaded regions are excluded by various experiments, while the region between the black lines is preferred by $(g-2)_\mu$.

$$(X_{N_1}, X_{N_2}, X_{N_3}) = (-1, 3, 7), \quad X_{Q_i, D_i, U_i} = -1, \quad (3.17)$$

$\tilde{L}_{\mu-\tau}$ model:

$$\begin{aligned} (X_{L_1}, X_{L_2}, X_{L_3}) &= (0, 7, -7), & (X_{E_1}, X_{E_2}, X_{E_3}) &= (-3, 8, -5), \\ (X_{N_1}, X_{N_2}, X_{N_3}) &= (5, 3, 8), & X_{Q_i, D_i, U_i} &= 0. \end{aligned} \quad (3.18)$$

Common for these models is that they have large vectorial coupling to the muons and only a small axial component, which then maximizes the NP contributions to the $(g-2)_\mu$ with the right sign to explain the anomaly. Both models also maintain a large ratio between the muon and electron charges, without which there is little hope of evading the Borexino bound (that the Borexino bound is relevant even for small induced couplings to electrons we saw already in the case of the $L_{\mu-\tau}$ model).

Even though the two models, $\tilde{L}-3B$ and $\tilde{L}_{\mu-\tau}$, were chosen such that they would avoid the most stringent bounds, it is clear from Fig. 4 that the Borexino and CCFR bounds are still strong enough to almost completely close the window on the region of parameter space that would lead to the explanation of the $(g-2)_\mu$ anomalies, assuming that the kinetic mixing vanishes in the UV.⁶ It would be interesting to relax the model search criteria beyond $|X_F| \leq 10$. We anticipate that this would generate additional feasible models with axial

⁶Note that we still use DARKCAST to draw the exclusion regions even though only contributions from vector couplings are implemented in it at present. While this captures the dominant contributions the correct bounds should be even slightly stronger than what is shown in Fig. 4.

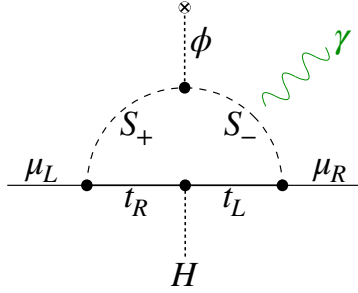


Figure 5. A muoquark model for the radiative muon mass generation that also contributes to the anomalous magnetic moment through the above diagram. See main text in Sec. 4 for further details.

currents that are further suppressed, and also have a larger muon-to-electron charge ratio, further relaxing the experimental bounds.

4 Muon mass and $(g - 2)_\mu$ at one loop

The observed smallness of Yukawa couplings can be explained in models in which fermion masses are generated from radiative corrections [154, 155]. Here we focus on radiatively generated muon mass. Since both the muon mass and the muon anomalous magnetic moment are chirality flipping operators, the TeV-scale NP that at one-loop generates the muon mass then generically also gives correlated one-loop NP contributions to $(g - 2)_\mu$ [156].

Model example

Let us consider a scenario in which the SM is extended by two scalar leptoquarks, S_+ and S_- , in the $(\mathbf{3}, \mathbf{2}, 7/6)$ representation of the SM gauge group. This leptoquark representation is usually called R_2 as in Ref. [75], however, for clarity we use a simpler notation in this section. We assume that the leptoquarks are coupled to the third generation quarks, q_L^3, t_R , and the second generation leptons, ℓ_L^2, μ_R . The model is assumed to have a Z_2 parity symmetry under which S_- and μ_R are odd, while all the other fields are even,

$$\mathcal{L} \supset \eta_L \bar{t}_R \ell_L^2 i\sigma_2 S_+ - \eta_R \bar{q}_L^3 \mu_R S_- + \text{H.c.} . \quad (4.1)$$

The global phase rotations can be used to make the couplings $\eta_{L,R}$ real without loss of generality. We assume that the left-handed quark doublet is defined in the down-quark mass eigenstate basis and take $V_{tb} = 1$.

The Z_2 symmetry forbids the direct muon Yukawa coupling, $\bar{\ell}_L^2 \tilde{H} \mu_R$. This is then generated only radiatively due to the presence of a Z_2 soft breaking term,

$$\mathcal{L}_{\text{break}} \supset -\tilde{m}_S^2 S_+^\dagger S_- + \text{H.c.} , \quad (4.2)$$

which induces a finite one-loop contribution to the muon mass as well as to the anomalous magnetic moment. For simplicity, we take the Z_2 symmetric mass terms,

$$\mathcal{L} \supset -m_{S_-}^2 S_-^\dagger S_- - m_{S_+}^2 S_+^\dagger S_+ , \quad (4.3)$$

to be degenerate, $m_S^2 \equiv m_{S_+}^2 = m_{S_-}^2$, with $0 < \tilde{m}_S^2 \ll m_S^2$. This induces maximal mixing, $\theta = \pi/4$, into the mass eigenstates $S_{1,2}$, with the corresponding physical masses given by $m_{S_{1(2)}}^2 = m^2 \mp \tilde{m}^2$. Furthermore, we assume that $m_t \ll m_S$ as suggested by the direct searches for leptoquarks at the LHC [157, 158].

Expanding the muon mass and the anomalous magnetic moment to the leading order in m_t/m_S and \tilde{m}_S/m_S (see [93, 155] for full expressions),

$$\begin{aligned} m_\mu &\approx \frac{3}{16\pi^2} m_t \eta_L \eta_R \frac{\tilde{m}_S^2}{m_S^2}, \\ \Delta a_\mu &\approx \frac{3}{16\pi^2} \eta_L \eta_R \frac{m_\mu m_t \tilde{m}_S^2}{m_S^4} \left(5 - 4Q_S + 2(1 - Q_S) \log \frac{m_t^2}{m_S^2} \right). \end{aligned} \quad (4.4)$$

Assuming that m_μ is entirely generated by the above one loop radiative correction, the ratio $\Delta a_\mu/m_\mu$ depends only on two unknowns, m_S and Q_S ,

$$\Delta a_\mu \approx \frac{m_\mu^2}{m_S^2} \left(5 - 4Q_S + 2(Q_S - 1) \log \frac{m_S^2}{m_t^2} \right). \quad (4.5)$$

Since Δa_μ needs to be positive, and $m_S \gg m_t$ experimentally, this puts a constraint on possible values of leptoquark charge, $Q_S \gtrsim 1$. In our example, the electric charge of the scalars running in the loop is $Q_S = 5/3$. Consequently, $\Delta a_\mu = (251 \pm 59) \times 10^{-11}$ points to $m_S \in [5 - 7]$ TeV. For $\eta_L \eta_R \approx 1$, the soft breaking mass needed to match the muon mass is then $\tilde{m}_S \approx 1$ TeV.

A wider parameter space opens up, if we move away from the limit $m_{S_+} \neq m_{S_-}$. Assuming as before that the muon mass is entirely due to the one loop radiative correction, Eq. (4.5) generalizes to [156]

$$\Delta a_\mu = \frac{m_\mu^2}{m_t^2} \tilde{F} \left(\frac{m_{S_1}^2}{m_t^2}, \frac{m_{S_2}^2}{m_t^2} \right), \quad (4.6)$$

where

$$\begin{aligned} \tilde{F}(x_1, x_2) &= \left(\frac{x_1 \log x_1}{1 - x_1} - \frac{x_2 \log x_2}{1 - x_2} \right)^{-1} \left[\frac{3x_1 - 1}{(1 - x_1)^2} - \frac{3x_2 - 1}{(1 - x_2)^2} + \frac{2x_1^2 \log x_1}{(1 - x_1)^3} \right. \\ &\quad \left. - \frac{2x_2^2 \log x_2}{(1 - x_2)^3} + 2Q_S \left(\frac{1}{1 - x_1} - \frac{1}{1 - x_2} + \frac{x_1 \log x_1}{(1 - x_1)^2} - \frac{x_2 \log x_2}{(1 - x_2)^2} \right) \right]. \end{aligned} \quad (4.7)$$

The preferred region in the S_1, S_2 mass plane, taking $Q_S = 5/3$, that explains the observed deviations in Δa_μ is shown in Fig. 6 as the brown shaded band.⁷

U(1)_X completion

The above scenario can be elegantly UV completed in our setup. The scan over the anomaly free charge assignments in Section 2 reveals a family of solutions for which the dimension-4

⁷We note in passing that requiring a positive contribution to Δa_μ even in this more general case still remains quite restrictive regarding the viable choices for the leptoquark gauge representations. In particular, the $(\bar{\mathbf{3}}, \mathbf{1}, 1/3)$ scalar leptoquark is not a phenomenologically viable possibility.

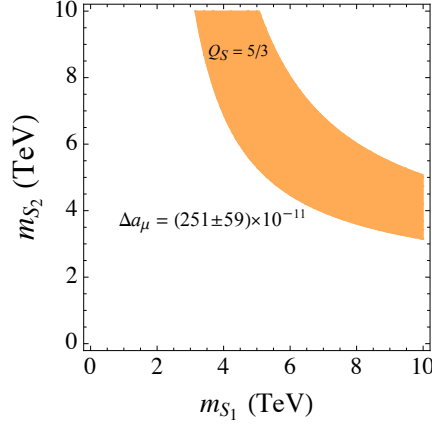


Figure 6. Preferred parameter space in the muoquark model for the radiative muon mass generation as implied by the $(g-2)_\mu$ anomaly. See the main text in Sec. 4 for further details.

muon Yukawa is forbidden. This occurs when the $U(1)_{X_\mu}$ charge of the left-handed muon is different from the charge of the right-handed muon. We assume that in addition to the SM there are three scalars, the S_\pm in the $(\mathbf{3}, \mathbf{2}, 7/6)$ representation of the SM gauge group and the SM singlet ϕ . The extra scalars carry the following charges under the $U(1)_{X_\mu}$ gauge symmetry

$$X_{S_+} = -X_{L_2} + X_{U_i} = -X_\mu + X_q, \quad (4.8)$$

$$X_{S_-} = -X_{E_2} + X_{Q_i} = -X_\mu - b_{E_2} + X_q, \quad (4.9)$$

$$X_\phi = -X_{S_-} + X_{S_+} = b_{E_2}. \quad (4.10)$$

where $X_q = (-X_e - X_\mu - X_\tau)/9$ (see Section 2.2.2). The leptoquarks $S_+(S_-)$ have allowed couplings to the left-(right-)handed muons, respectively, i.e., they are the muoquarks. An explicit mass mixing between S_+ and S_- is forbidden by the $U(1)_{X_\mu}$ gauge symmetry. However, there is a gauge invariant trilinear scalar coupling

$$\mathcal{L} \supset -A\phi S_+^\dagger S_- + \text{H.c.}, \quad (4.11)$$

that gives rise to the $U(1)_{X_\mu}$ mass mixing term, $\tilde{m}_S^2 = Av_\phi$, once the SM singlet ϕ gets a VEV, $\langle\phi\rangle = v_\phi$ and breaks $U(1)_{X_\mu}$ spontaneously. The radiative generation of the muon mass requires a single insertion of v_ϕ , a mechanism that is illustrated by the Feynman diagram in Fig. 5. An alternative charge assignment for ϕ can be $X_\phi = b_{E_2}/2$, in which case the quartic interaction $\mathcal{L} \supset -\lambda\phi^2 S_+^\dagger S_-$ is gauge invariant, giving $\tilde{m}_S^2 = \lambda v_\phi^2$ and the radiative generation of the muon mass is induced by two insertions of the ϕ VEV.

In the above set-up the X_μ gauge boson is no longer needed to resolve $(g-2)_\mu$ and can be decoupled from the phenomenological discussion by taking the small gauge coupling limit. In addition, the corrections to the $h \rightarrow \mu^+\mu^-$ decays start at $\mathcal{O}(m_t^2/m_S^2)$ and are well within the present experimental bounds on the Higgs couplings to muons.

Field	SU(5)	SU(3)'	SU(2) _L	U(1)'
ℓ_L^1	1	1	2	-1/2
e_R^1	1	1	1	-1
q_L^i	1	3	2	1/6
u_R^i	1	3	1	2/3
d_R^i	1	3	1	-1/3
ψ_L	5	1	2	-1/10
ψ_R^+	5	1	1	2/5
ψ_R^-	5	1	1	-3/5

Table 2. Quantum numbers of SM-like fermions under the G_{5321} gauge symmetry; $i \in \{1, 2\}$.

5 A vector muoquark model

For a leptoquark to become a muoquark, it has to be charged under a $U(1)_X$ gauge symmetry discussed in Section 2. While this is straightforward for a scalar leptoquark, charging a vector leptoquark in a UV complete model is more challenging. In this section, we demonstrate that it is possible to construct UV-complete gauge models in which a vector leptoquark carries a $U(1)_X$ charge. We build a model that contains a U_1 muoquark with the SM quantum numbers $(\mathbf{3}, \mathbf{1}, 2/3)$ as one of the leptoquarks charged under the gauged $U(1)_{\mu-\tau}$ as an example.

Gauge group and fermion embedding

We consider the gauge group

$$G_{5321} = \text{SU}(5) \times \text{SU}(3)' \times \text{SU}(2)_L \times \text{U}(1)' \quad (5.1)$$

and embed the third generation of quarks together with the second and third lepton generations into fundamental $\mathbf{5}$ multiplets of $\text{SU}(5)$:

$$\psi_L \sim (q_L^3 \ell_L^3 \ell_L^2)^\top, \quad \psi_R^+ \sim (u_R^3 \nu_R^3 \nu_R^2)^\top, \quad \psi_R^- \sim (d_R^3 e_R^3 e_R^2)^\top. \quad (5.2)$$

The quantum numbers of all SM-like fermions are collected in Table 2. Even though the $\text{SU}(5)$ multiplets unify fields from different fermion generations, all gauge anomalies cancel. The $\text{SU}(5)$ group contains the subgroup $\text{SU}(3)_5 \times \text{U}(1)_5 \times \text{U}(1)_{\mu-\tau} \subset \text{SU}(5)$ under which the $\mathbf{5}$ decomposes as

$$\mathbf{5} \rightarrow (\mathbf{3}, 4/15, 0) \oplus (\mathbf{1}, -2/5, -1) \oplus (\mathbf{1}, -2/5, 1), \quad (5.3)$$

i.e. there is one $\text{SU}(3)_5$ triplet that is uncharged under $U(1)_{\mu-\tau}$ and is identified with a third-generation quark, as well as two $\text{SU}(3)_5$ singlets charged under $U(1)_{\mu-\tau}$ that are identified with third and second generation leptons. The QCD and hypercharge gauge groups are given by the diagonal subgroups of $\text{SU}(3)_5 \times \text{SU}(3)'$ and $\text{U}(1)_5 \times \text{U}(1)'$, respectively,

$$\text{SU}(3)_c = [\text{SU}(3)_5 \times \text{SU}(3)']_{\text{diag}}, \quad \text{U}(1)_Y = [\text{U}(1)_5 \times \text{U}(1)']_{\text{diag}}. \quad (5.4)$$

It can be easily verified that the sums of $U(1)'$ charges in Table 2 and $U(1)_5$ charges in Eq. (5.3) yield the correct hypercharges, see also Appendix C.

Gauge sector and vector bosons

There are different ways to break $G_{5321} \rightarrow G_{\text{SM}} \times U(1)_{\mu-\tau}$ that result in different vector boson spectra. In particular, there are two possible intermediate gauge groups:

- $G_{\text{SM}} \times \text{SU}(2)_{\mu\tau}$

In this case, the breaking $G_{5321} \rightarrow G_{\text{SM}} \times U(1)_{\mu-\tau}$ is done in the following two steps.

1. $G_{5321} \rightarrow G_{\text{SM}} \times \text{SU}(2)_{\mu\tau}$

This first step proceeds via the $\text{SU}(5)$ subgroup $\text{SU}(3)_5 \times \text{SU}(2)_{\mu\tau} \times \text{U}(1)_5 \subset \text{SU}(5)$, under which the fundamental **5** and the adjoint **24** representations decompose as

$$\begin{aligned} \mathbf{5} &\rightarrow (\mathbf{3}, \mathbf{1}, 4/15) \oplus (\mathbf{1}, \mathbf{2}, -2/5), \\ \mathbf{24} &\rightarrow (\mathbf{1}, \mathbf{1}, 0) \oplus (\mathbf{8}, \mathbf{1}, 0) \oplus (\mathbf{1}, \mathbf{3}, 0) \oplus (\mathbf{3}, \mathbf{2}, 2/3) \oplus (\bar{\mathbf{3}}, \mathbf{2}, -2/3), \end{aligned} \quad (5.5)$$

such that the third and second lepton generations are contained in doublets of $\text{SU}(2)_{\mu\tau}$. After this step, the spectrum of massless gauge bosons consists of the SM gauge bosons and an additional triplet of the unbroken $\text{SU}(2)_{\mu\tau}$. The vector bosons that become massive by this breaking and their quantum numbers under $\text{SU}(3)_c \times \text{SU}(2)_L \times \text{U}(1)_Y \times \text{SU}(2)_{\mu\tau}$ are

- $G'_\mu \sim (\mathbf{8}, \mathbf{1}, 0; \mathbf{1})$, a heavy gluon-like vector boson also known as *coloron*,
- $B'_\mu \sim (\mathbf{1}, \mathbf{1}, 0; \mathbf{1})$, a heavy B -boson-like neutral vector boson,
- $U_\mu \sim (\mathbf{3}, \mathbf{1}, 2/3; \mathbf{2})$ (and its complex conjugate), an $\text{SU}(2)_L$ singlet vector leptoquark known as U_1 , coming in a doublet of $\text{SU}(2)_{\mu\tau}$.

2. $\text{SU}(2)_{\mu\tau} \rightarrow \text{U}(1)_{\mu-\tau}$

In this second step, the **2** of $\text{SU}(2)_{\mu\tau}$ decompose under $\text{U}(1)_{\mu-\tau}$ as

$$\mathbf{2} \rightarrow -1 \oplus 1, \quad (5.6)$$

such that the τ and μ leptons inside the $\text{SU}(2)_{\mu\tau}$ doublets receive $\text{U}(1)_{\mu-\tau}$ charges -1 and $+1$, respectively. Similarly, the $\text{SU}(2)_{\mu\tau}$ doublet of U_1 leptoquarks splits into two leptoquarks with $\text{U}(1)_{\mu-\tau}$ charges -1 and $+1$. Furthermore, the vector bosons in the $\text{SU}(2)_{\mu\tau}$ triplet that mediate τ - μ transitions become massive, while the one related to the diagonal $\text{SU}(2)_{\mu\tau}$ generator becomes the gauge boson of $\text{U}(1)_{\mu-\tau}$.

- $\text{SU}(4)_5 \times \text{U}(1)_{5'} \times \text{SU}(3)' \times \text{SU}(2)_L \times \text{U}(1)'$

The breaking $G_{5321} \rightarrow G_{\text{SM}} \times \text{U}(1)_{\mu-\tau}$ is again done in two steps:

1. $G_{5321} \rightarrow \text{SU}(4)_5 \times \text{U}(1)_{5'} \times \text{SU}(3)' \times \text{SU}(2)_L \times \text{U}(1)'$

This breaking proceeds via the $SU(5)$ subgroup $SU(4)_5 \times U(1)_{5'} \subset SU(5)$, under which the fundamental $\mathbf{5}$ and the adjoint $\mathbf{24}$ representations decompose as⁸

$$\begin{aligned}\mathbf{5} &\rightarrow (\mathbf{4}, 1/10) \otimes (\mathbf{1}, -2/5), \\ \mathbf{24} &\rightarrow (\mathbf{1}, 0) \oplus (\mathbf{15}, 0) \oplus (\mathbf{4}, 1/2) \oplus (\bar{\mathbf{4}}, -1/2),\end{aligned}\tag{5.7}$$

such that the third generation leptons stay unified with the third generation quarks in the $\mathbf{4}$ of $SU(4)_5$, while the second generation leptons are singlets of $SU(4)_5$. The vector bosons that become massive in this step and their quantum numbers under $SU(4)_5 \times U(1)_{5'} \times SU(3)' \times SU(2)_L \times U(1)'$ are

- $V_\mu \sim (\mathbf{4}, 1/2; \mathbf{1}, \mathbf{1}, 0)$ (and its complex conjugate), which contains the U_1 leptoquark that couples second generation leptons to third generation quarks as well as the SM neutral vector bosons that mediate τ - μ transitions.

2. $SU(4)_5 \times U(1)_{5'} \times SU(3)' \times U(1)' \rightarrow SU(3)_c \times U(1)_Y \times U(1)_{\mu-\tau}$

This breaking proceeds via the $SU(4)_5$ subgroup $SU(3)_4 \times U(1)_4 \subset SU(4)_5$, under which the $\mathbf{4}$ decomposes as⁹

$$\mathbf{4} \rightarrow (\mathbf{3}, 1/6) \oplus (\mathbf{1}, -1/2).\tag{5.8}$$

The $U(1)_{\mu-\tau}$ generator $X_{\mu-\tau}$ and the hypercharge generator Y are given by the linear combinations of the generators $X_{5'}$, X_4 , and X_1 of $U(1)_{5'}$, $U(1)_4$, and $U(1)'$ as

$$X_{\mu-\tau} = \frac{3}{2} X_4 - \frac{5}{2} X_{5'}, \quad Y = X_4 + X_{5'} + X_1.\tag{5.9}$$

The vector bosons that become massive in this step and their quantum numbers under $SU(3)_c \times SU(2)_L \times U(1)_Y \times U(1)_{\mu-\tau}$ are:

- $G'_\mu \sim (\mathbf{8}, \mathbf{1}, 0, 0)$, a heavy gluon-like “coloron”,
- $B'_\mu \sim (\mathbf{1}, \mathbf{1}, 0, 0)$, a heavy B -boson-like neutral vector boson,
- $U_\mu^{(\tau)} \sim (\mathbf{3}, \mathbf{1}, 2/3, 1)$ (and its complex conjugate), a U_1 leptoquark coupling third generation leptons to third generation quarks.

In addition, the heavy vector boson four-plet V_μ splits into $(\mathbf{3}, \mathbf{1}, 2/3, -1) \oplus (\mathbf{1}, \mathbf{1}, 0, 2)$, which is the U_1 leptoquark coupling second generation leptons to third generation quarks and the SM neutral vector that mediates τ - μ transitions.

6 Conclusions

Lepton-flavored $U(1)_X$ gauge extensions of the SM — the focus of this work — provide a framework in which the first experimental deviations are expected to be seen in the lepton flavor universality violating (LFUV) observables and not, as is more common in many other new physics models, in the lepton flavor violating (LFV) observables. The $U(1)_X$ extensions of the SM are especially interesting in view of the recent flavor anomalies, showing hints of

⁸The generator $X_{5'}$ of $U(1)_{5'}$ is given in terms of the $SU(5)$ generators T_5 as $X_{5'} = \frac{2}{\sqrt{10}} T_5^{24}$.

⁹The generator X_4 of $U(1)_4$ is given in terms of the $SU(4)_5$ generators T_4 as $X_4 = \frac{2}{\sqrt{6}} T_4^{15}$.

new physics in LFUV ratios $R_{K^{(*)}}$, while the LFV transitions such as the $\tau \rightarrow 3\mu$ decay are absent. In the $U(1)_X$ models the LFUV is hardcoded in the X_μ gauge boson interactions through generation-dependent charges (allowing, e.g., for the muonic force). In contrast, the LFV is forbidden in the infrared-relevant operators. The LFV effects arise only in the form of higher-dimensional operators, whose effects are power suppressed by high-energy scales.

The bulk of the present manuscript dealt with different SM+ $3\nu_R$ anomaly-free charge assignments and their impact on the model building applications for the flavor physics anomalies involving muons: $(g-2)_\mu$ and anomalies in rare B -meson decays ($R_{K^{(*)}}$ and $b \rightarrow s\mu^+\mu^-$ angular distributions and branching ratios). Our main finding is that the quark flavor universal, but lepton flavor non-universal, $U(1)_X$ gauge symmetry extensions provide a natural framework for the introduction of a leptoquark coupled to a single lepton flavor. Our attention here is on the TeV-scale *muoquarks* — leptoquarks that due to their $U(1)_X$ charges are allowed to couple to muons but not to electrons and taus. We require the cancellation of the chiral anomalies within the field content present at low-energies, i.e., already within the SM+ $3\nu_R$. This guarantees the theory to be consistent without introducing additional $U(1)_X$ charged fields in the UV.

Our work builds on and extends the simple scenario for flavor anomalies that was first proposed in Ref. [1]. Extending the SM gauge group by an additional $B-3L_\mu$ gauge symmetry was found to have two desirable effects. Firstly, it guaranteed that the S_3 scalar muoquark, needed to explain the anomalies in rare B decays through tree-level contributions, does not have LFV couplings. Secondly, the existence of the gauge boson X_μ gives a natural explanation of the $(g-2)_\mu$ anomaly through a one loop contribution. The $B-3L_\mu$ gauge group is by far not the only choice one can make. In this manuscript we identified 273 inequivalent models supporting the muoquark when demanding that the ratio of maximal to minimal $U(1)_X$ charges is at most equal to ten. As shown in Section 2 one can classify the $U(1)_X$ models into two broad categories based on whether or not for all three generations the dimension-4 lepton Yukawa interaction are allowed by the $U(1)_X$ charges.

In the rest of the manuscript we showed three different uses for the $U(1)_X$ model classifications. The first question we addressed is how restricted are the new physics models that use a light X_μ vector boson to explain the $(g-2)_\mu$ via one loop contributions (while at the same time explaining the anomalies in rare B decays through tree level leptoquark exchanges). The naive expectation was that the constraints on X_μ couplings to quarks and leptons are so severe that only very few examples, such as the widely popular $L_\mu-L_\tau$ model, would remain viable. To our surprise we instead found that there are many charge assignments that lead to phenomenologically viable explanations of the $(g-2)_\mu$ anomaly, including the models with couplings to electrons and/or to light quarks (see Section 3 for further details and several benchmark models).

Another application of the lepton-flavored $U(1)_X$ is in the models of radiative muon mass generation that can simultaneously lead to the explanation of the $(g-2)_\mu$ anomaly. The models with two TeV-scale leptoquarks exhibiting a parity symmetry were already known to realize such a scenario. We point out that the parity symmetry can be an automatic consequence of the $U(1)_X$ gauge symmetry. The mixing between the scalars is then generated once the $U(1)_X$ becomes spontaneously broken. Further details on such scenarios are given

in Section 4.

Our final application concerns the conundrum that whereas scalar leptoquarks are easily charged under the $U(1)_X$ the vector leptoquarks are not. In Section 5 we settle the question whether or not it is even possible to have a vector muoquark in a perturbative UV complete framework. For this purpose we built a proof-of-principle UV complete gauge model for the Pati-Salam vector leptoquark, carrying a nonzero muon number.

In conclusion, the lepton-flavored $U(1)_X$ extensions of the SM provide a powerful framework to address the current flavor anomalies. There is a variety of mediators to be considered, such as light or heavy gauge bosons X_μ , heavy scalar-, or vector-leptoquarks. The richness of the phenomenology such extensions entail is apparent from the large number of possible chiral-anomaly-free charge assignments. Within the present work we probably only scratched the surface of possibilities. One can imagine several different interesting future research directions. As shown in Ref. [1], the minimal realization of the neutrino masses imposes nontrivial requirements on the model building. Having a more complete study of implications from $U(1)_X$ gauge symmetry on the neutrino sector would be highly desirable. Another open question is what would be the result of relaxing assumption about the cancellations of anomalies in the IR, allowing instead for chiral fermions that obtain the mass from $U(1)_X$ breaking vacuum expectation values. We anticipate that many, if not all, of the possible models can be successfully probed experimentally, since the parameter space of interest for explaining the $(g-2)_\mu$ anomaly is mostly within reach of the next generation experiments.

Acknowledgments

We thank Philip Ilten for updating the DARKCAST in time for the updated version to be used in this work. We also thank Joe Davighi, Javier Fuentes-Martin and Ben Stefanek for useful discussions. The work of AG and AET has received funding from the Swiss National Science Foundation (SNF) through the Eccellenza Professorial Fellowship ‘‘Flavor Physics at the High Energy Frontier’’ project number 186866. The work of AG is also partially supported by the European Research Council (ERC) under the European Union’s Horizon 2020 research and innovation programme, grant agreement 833280 (FLAY). The work of PS is supported by the SNF grant 200020175449/1. The work of YS is supported by grants from the United States-Israel Binational Science Foundation (BSF) (NSF-BSF program grant No. 2018683), by the Israel Science Foundation (grant No. 482/20) and by the Azrieli foundation. YS is Taub fellow (supported by the Taub Family Foundation). JZ acknowledges support in part by the DOE grant de-sc0011784.

A Kinetic mixing

A.1 Equivalence of charge assignments

For a gauge group with multiple Abelian factors, there is a continuum of physically equivalent choices for the products of $U(1)$ subgroups. The freedom in defining the Abelian factors

then translates into a continuum of physically equivalent charge assignments for the matter field representations.

To demonstrate the equivalence of the charge assignments, let us consider a toy model consisting of a $U(1)^n = U(1)_1 \times \dots \times U(1)_n$ gauge group, with associated gauge fields A_i^μ , $i = 1, \dots, n$, and a set of matter field $\{f\}$ (fermions and/or scalars) carrying charges q_i^f under group $U(1)_i$. It is useful to absorb the gauge couplings into the definition of the gauge fields so that the kinetic term and the covariant derivative are given respectively by (see, e.g., Ref. [159])

$$\mathcal{L} \supset -\frac{1}{4}F_{i\mu\nu}h_{ij}^{-1}F_j^{\mu\nu}, \quad D_\mu^f = \partial_\mu - iq_i^f A_{i\mu}. \quad (\text{A.1})$$

All the information on the gauge couplings and kinetic mixing parameters is contained in the symmetric, positive-definite matrix h .

Consider now the effect of a linear field transformation $A_i^\mu \rightarrow L_{ij}A_j^\mu$, where $L \in \mathbb{R}^{n \times n}$ is invertible. The kinetic term and the covariant derivative expressed in terms of the transformed fields are given by

$$\mathcal{L} \supset -\frac{1}{4}F_{i\mu\nu}\tilde{h}_{ij}^{-1}F_j^{\mu\nu}, \quad D_\mu^f = \partial_\mu - i\tilde{q}_i^f A_{i\mu}, \quad (\text{A.2})$$

where the new coupling matrix $\tilde{h} = L^{-1}h(L^{-1})^\top$ is still positive-definite due to invertibility of L , ensuring the validity of the transformed theory. The matter charges are also linearly transformed, $\tilde{q}^f = L^\top q^f$. Since the field redefinitions give physically equivalent theories, the linear transformations L_{ij} give a family of physically equivalent choices for the definitions of $U(1)$ factors, with appropriately transformed matter field charges. We limit ourselves to rational charges, thus $L \in \mathbb{Q}^{n \times n}$.

A.2 Mass basis of the gauge sector

We next turn to the example at hand, the SM supplemented by the $U(1)_X$ gauge group. To determine the mass eigenstates in the neutral gauge boson sector, it suffices to focus on the $SU(2)_L \times U(1)_Y \times U(1)_X$ subgroup. We assume that the $U(1)_X$ is spontaneously broken by a VEV of a SM singlet, resulting in a mass term, $\frac{1}{2}m_X^2 X_\mu^2$, but can otherwise remain agnostic about the specifics of the $U(1)_X$ breaking sector. That is, the part of the Lagrangian describing the EW and X_μ gauge interactions is, after $U(1)_X$ breaking, given by

$$\begin{aligned} \mathcal{L} \supset & -\frac{1}{4}B_{\mu\nu}^2 - \frac{1}{4}X_{\mu\nu}^2 + \frac{1}{2}\varepsilon B_{\mu\nu}X^{\mu\nu} - \frac{1}{4}(W_{\mu\nu}^a)^2 + |D_\mu H|^2 + \frac{1}{2}m_X^2 X_\mu^2 \\ & + g_1 B_\mu J_Y^\mu + g_2 W_\mu^a J_W^{a\mu} + g_X X_\mu J_X^\mu, \end{aligned} \quad (\text{A.3})$$

where $J_{X,Y,W}^\mu$ are the respective fermion currents. After EW symmetry breaking due to the SM Higgs VEV the above Lagrangian is,

$$\begin{aligned} \mathcal{L} \supset & -\frac{1}{4}(A_{\mu\nu}^2 + X_{\mu\nu}^2 + Z_{\mu\nu}^2) + \frac{1}{2}\varepsilon (c_w A_{\mu\nu} - s_w Z_{\mu\nu})X^{\mu\nu} + \frac{1}{2}M_Z^2 Z_\mu^2 + \frac{1}{2}m_X^2 X_\mu^2 \\ & + e A_\mu J_{\text{EM}}^\mu + g_Z Z_\mu J_Z^\mu + g_X X_\mu J_X^\mu, \end{aligned} \quad (\text{A.4})$$

where Z_μ, A_μ are the would be mass eigenstates had we had only the SM gauge group and are given by $B_\mu = c_w Z_\mu - s_w A_\mu$ and $W_\mu^3 = c_w Z_\mu + s_w A_\mu$, where $c_w \equiv \cos \theta_w$, $s_w \equiv \sin \theta_w$

with θ_w the weak mixing angle. Also, $g_Z = \sqrt{g_1^2 + g_2^2}$ is the usual coupling constant of the Z_μ . A non-unitary transformation of the fields,

$$A \longrightarrow A + \frac{c_w \varepsilon}{r_\varepsilon} X, \quad Z \longrightarrow Z - \frac{s_w \varepsilon}{r_\varepsilon} X, \quad \text{and} \quad X \longrightarrow \frac{1}{r_\varepsilon} X, \quad r_\varepsilon = \sqrt{1 - \varepsilon^2}, \quad (\text{A.5})$$

eliminates the kinetic-mixing terms:

$$\begin{aligned} \mathcal{L} \supset & -\frac{1}{4}(A_{\mu\nu}^2 + X_{\mu\nu}^2 + Z_{\mu\nu}^2) + \frac{M_Z^2}{2} \left(Z_\mu - \frac{s_w \varepsilon}{r_\varepsilon} X_\mu \right)^2 + \frac{m_X^2}{2r_\varepsilon^2} X_\mu^2 \\ & + e A_\mu J_{\text{EM}}^\mu + g_Z Z_\mu J_Z^\mu + \frac{1}{r_\varepsilon} X_\mu (g_X J_X^\mu + c_w \varepsilon e J_A^\mu - s_w \varepsilon g_Z J_Z^\mu). \end{aligned} \quad (\text{A.6})$$

For $\varepsilon \ll 1$, a rotation by $s_w \varepsilon$ between Z and X suffices to mass-diagonalize the Lagrangian up to subleading terms, giving (in a slightly abused notation with Z_μ, X_μ now denoting the rotated fields)

$$\begin{aligned} \mathcal{L} \supset & -\frac{1}{4}(A_{\mu\nu}^2 + X_{\mu\nu}^2 + Z_{\mu\nu}^2) + \frac{1}{2} M_Z^2 Z_\mu^2 + \frac{1}{2} m_X^2 X_\mu^2 \\ & + e A_\mu J_{\text{EM}}^\mu + g_Z Z_\mu J_Z^\mu + X_\mu (g_X J_X^\mu + c_w \varepsilon e J_A^\mu) \\ & + \mathcal{O}(g_X \varepsilon, \varepsilon^2, \varepsilon m_X^2 / M_Z^2). \end{aligned} \quad (\text{A.7})$$

The result is that the effective $U(1)_X$ charge of the matter fields is

$$q_X^{\text{eff}} = q_X + \frac{c_w e \varepsilon}{g_X} q_{\text{EM}}, \quad (\text{A.8})$$

where q_{EM} is the ordinary EM charge.

A.3 The RG running of the kinetic mixing parameter

The 1-loop running of the kinetic mixing parameter, as in Eq. (A.3), is given by [159]

$$\frac{d\varepsilon}{dt} = \frac{g_1 g_X}{48\pi^2} \left[2s_{BX} + s_{BB} \varepsilon \frac{g_1}{g_X} + s_{XX} \varepsilon \frac{g_X}{g_1} \right], \quad t = \ln \frac{\mu}{\mu_0}, \quad (\text{A.9})$$

with μ the renormalization scale, and μ_0 the starting scale for RG running, to be taken $\mu_0 = 3$ TeV in the numerics below. The coefficients s_{xy} are determined by the charges of the matter fields of the model. We have

$$s_{xy} = 2 \text{Tr}_F [Q_x Q_y] + \text{Tr}_S [Q_x Q_y], \quad (\text{A.10})$$

with the two traces running over the Weyl-spinor and complex-scalar degrees of freedom, respectively. For SM+ $3\nu_R$ with an S_3 muoquark the coefficients in the RG equation (A.9) are

$$\begin{aligned} s_{BB} &= \frac{43}{2}, \quad s_{BX} = 12X_q - 3(X_q + X_{L_2}) - 2 \sum_i (X_{L_i} + X_{E_2}), \\ s_{XX} &= 72X_q^2 + 9(X_q + X_{L_2})^2 + 2 \sum_i [2X_{L_i}^2 + X_{E_i}^2 + X_{N_i}^2]. \end{aligned} \quad (\text{A.11})$$

In the models we consider the contribution from s_{XX} is numerically negligible.

The 1-loop RGE can be integrated analytically in the $g_X, \varepsilon \ll g_B$ limit. The g_X gauge coupling can be treated as a constant to a very good approximation, since

$$\frac{dg_X}{dt} = \mathcal{O}(g_X \varepsilon^2, g_X^2 \varepsilon, g_X^3). \quad (\text{A.12})$$

The running of the hypercharge coupling is given by

$$\frac{dg_1}{dt} = \frac{s_{BB}}{48\pi^2} g_1^3 + \mathcal{O}(g_X \varepsilon) \implies g_1(t) = \frac{\sqrt{24\pi^2/s_{BB}}}{\sqrt{T-t}}, \quad T = \frac{24\pi^2}{s_{BB} g_1^2(0)}, \quad (\text{A.13})$$

with $g_1(0)$ is the value of hypercharge coupling constant at scale μ_0 . The running of ε is driven by the hypercharge and integrates to

$$\varepsilon = \frac{\sqrt{T}\varepsilon_0 + bt}{\sqrt{T-t}}, \quad \text{where } b = \frac{g_1 s_{BX}}{\sqrt{24\pi^2 s_{BB}}}. \quad (\text{A.14})$$

For RG running from the leptoquark mass scale, $\mu_0 = 3 \text{ TeV}$, to the Planck mass, $M_{\text{Pl}} \simeq 1.2 \cdot 10^{19} \text{ GeV}$, we have $T \simeq 85$, while $t_{\text{Pl}} = 36$. To a reasonable approximation, we have

$$\varepsilon(M_{\text{Pl}}) - \varepsilon(\mu_0) \simeq 0.32\varepsilon(\mu_0) + 0.072s_{BX} g_X. \quad (\text{A.15})$$

B The X boson phenomenology

B.1 Neutrino trident limits

In this Appendix we show how to reinterpret the neutrino trident bounds from [48] relevant for Section 3.2. In the $q_A = 0, q_V = 1$ case of Ref. [48], it is possible to rescale the coupling g_X such that either the interference term or the pure NP contribution takes the form of the more general case of Eq. (3.6). To this end, it is convenient to rewrite this equation as

$$|\mathcal{M}_{\nu\mu\gamma}|^2 = |\mathcal{M}_0|^2 \left[(C_V^{\text{SM}})^2 + (C_A^{\text{SM}})^2 - 2 C_V^{\text{SM}} \mathcal{K}^{\text{inter}} \frac{m_X^2}{k^2 - m_X^2} + \mathcal{K}^X \left(\frac{m_X^2}{k^2 - m_X^2} \right)^2 \right], \quad (\text{B.1})$$

where the model-dependent contributions to the interference term and the pure NP term are encoded in

$$\mathcal{K}^{\text{inter}} = C_V^X + \frac{C_A^{\text{SM}}}{C_V^{\text{SM}}} C_A^X \quad \text{and} \quad \mathcal{K}^X = (C_V^X)^2 + (C_A^X)^2. \quad (\text{B.2})$$

In Ref. [48], these contributions are simply given by

$$\mathcal{K}_{[48]}^{\text{inter}} = g_X^2 \frac{v_{\text{SM}}^2}{m_X^2} \quad \text{and} \quad \mathcal{K}_{[48]}^X = g_X^4 \frac{v_{\text{SM}}^4}{m_X^4}. \quad (\text{B.3})$$

Consequently, the rescaling of g_X in Eq. (B.3) that yields the exact $\mathcal{K}^{\text{inter}}$ of the general case is given by

$$g_X^2 \rightarrow g_X^2 q_V^2 \left(1 + \frac{q_A}{q_V} \right) \left(1 + \frac{C_A^{\text{SM}}}{C_V^{\text{SM}}} \frac{q_A}{q_V} \right), \quad (\text{B.4})$$

such that the pure NP contribution \mathcal{K}^X receives an additional (wrong) term

$$\begin{aligned}\Delta\mathcal{K}^X &= 2 \frac{C_A^{\text{SM}}}{C_V^{\text{SM}}} C_A^X C_V^X \left(1 - \frac{1}{2} \left(\frac{C_V^{\text{SM}}}{C_A^{\text{SM}}} - \frac{C_A^{\text{SM}}}{C_V^{\text{SM}}} \right) \frac{C_A^X}{C_V^X} \right) \\ &\approx 1.1 C_A^X C_V^X \left(1 - 0.7 \frac{C_A^X}{C_V^X} \right).\end{aligned}\tag{B.5}$$

On the other hand, the rescaling of g_X in Eq. (B.3) that yields the exact \mathcal{K}^X of the general case is

$$g_X^2 \rightarrow g_X^2 q_V^2 \left(1 + \frac{q_A}{q_V} \right) \sqrt{1 + \frac{q_A}{q_V}},\tag{B.6}$$

such that the interference term $\mathcal{K}^{\text{inter}}$ receives an additional (wrong) term

$$\begin{aligned}\Delta\mathcal{K}^{\text{inter}} &= \sqrt{(C_V^X)^2 + (C_A^X)^2} - C_V^X - \frac{C_A^{\text{SM}}}{C_V^{\text{SM}}} C_A^X \\ &\approx -\frac{C_A^{\text{SM}}}{C_V^{\text{SM}}} C_A^X \left(1 - \frac{1}{2} \frac{C_V^{\text{SM}}}{C_A^{\text{SM}}} \frac{C_A^X}{C_V^X} \right) \approx -0.5 C_A^X \left(1 - 0.9 \frac{C_A^X}{C_V^X} \right).\end{aligned}\tag{B.7}$$

In the last line we used that, in order to explain $(g-2)_\mu$, in the region of interest one has $|q_V| > \sqrt{5}|q_A|$ and thus $C_V^X > 0$ and $(C_A^X/C_V^X)^2 \ll 1$. The interference with the SM is then constructive and furthermore $\text{sgn}(\Delta\mathcal{K}^{\text{inter}}) = -\text{sgn}(\Delta\mathcal{K}^X) = \text{sgn}(C_A^X)$. We therefore find that, when the two rescalings in Eqs. (B.4) and (B.6) are used to recast the bound on g_X from [48], one of them always gives an overestimation and the other always an underestimation of the true bound on g_X . In the NP models we consider, the difference between the two bounds is of the order of $\mathcal{O}(10\%)$, and thus an approximate recast by (B.4) and (B.6) is sufficiently accurate for our purposes. In the figures we show both bounds.

B.2 Decay channels

In Fig. 7 we plot for clarity the branching ratios of the X_μ boson for several final states as a function of the X_μ mass m_X derived with DARKCAST. The two benchmark models are presented in Section 3.5.1 and Section 3.5.2.

B.3 $R_{K^{(*)}}$ from a light X_μ vector boson

Here we extend the discussion given in Section 3.4 regarding the predictions for $R_{K^{(*)}}$ in the presence of a light vector boson X_μ . The $R_{K^{(*)}}$ observables are measured in bins of the invariant dilepton mass squared q^2 , and are given in terms of the q^2 -differential branching ratios by

$$R_{K^{(*)}}^{[q_{\min}^2, q_{\max}^2]} = \frac{\int_{q_{\min}^2}^{q_{\max}^2} dq^2 \frac{d\text{BR}(B \rightarrow K^{(*)} \mu^+ \mu^-)}{dq^2}}{\int_{q_{\min}^2}^{q_{\max}^2} dq^2 \frac{d\text{BR}(B \rightarrow K^{(*)} e^+ e^-)}{dq^2}}.\tag{B.8}$$

In the SM and for heavy NP particles, the differential branching ratios can be expressed as

$$\frac{d\text{BR}(B \rightarrow K^{(*)} \ell^+ \ell^-)}{dq^2} \simeq \text{Re} \sum_{i,j} f_{ij}(q^2) C_i C_j^*,\tag{B.9}$$

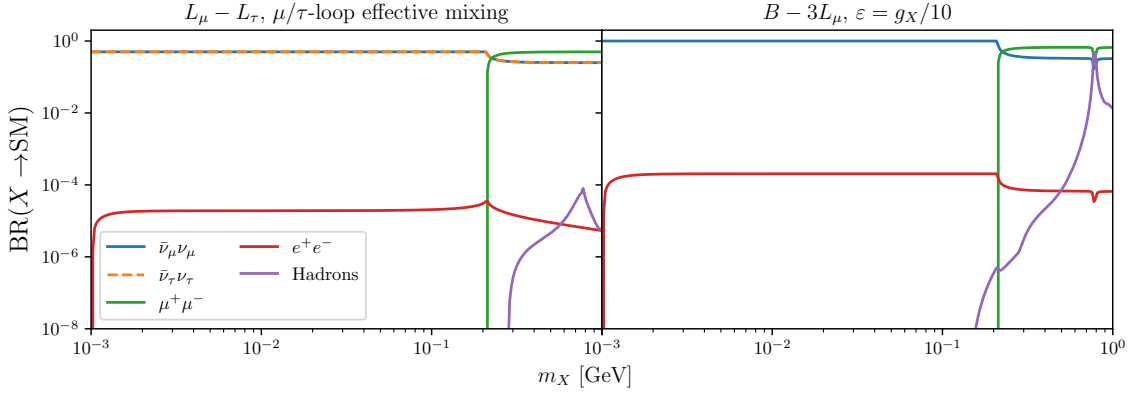


Figure 7. The X boson decay branching ratios in $L_\mu - L_\tau$ model (left) and $B - 3L_\mu$ model (right).

where $f_{ij}(q^2)$ are q^2 -dependent functions that depend on the parameters such as meson masses and hadronic form factors, while C_i denote the q^2 -independent Wilson coefficients of effective operators in the weak Hamiltonian. In the presence of a light NP mediator, its tree level effect can be modeled by introducing q^2 -dependent Wilson coefficients. In particular, the Wilson coefficients most relevant in the presence of the Lagrangian Eq. (3.8) are given in Eq. (3.9) and repeated here for convenience,

$$C_{9,10}^{(i)}(q^2) = \frac{q_{V,A}}{N} \frac{g_X g_{L(R)}^{bs}}{q^2 - m_X^2 + im_X \Gamma_X}. \quad (\text{B.10})$$

It is evident that due to these Wilson coefficients, the q^2 dependence of the differential branching ratios, and thus the value of the integrals in Eq. (B.8), strongly depends on the mass m_X . To demonstrate this, we show in the upper panel of Fig. 8 the minimal value of $R_K^{[1,1,6]}$ that can be obtained using the Wilson coefficients in Eq. B.10 for different masses m_X and different widths Γ_X . We have fixed $q_V = 1$, $q_A = 0$, $g_R^{bs} = 0$, $g_L^{bs} = 0.7 \times 10^{-8} \frac{m_X}{\text{GeV}}$ (cf. Eq. (3.10)), but kept g_X as a free parameter. The lower panel in Fig. 8 shows the g_X values that correspond to the minimal values of $R_K^{[1,1,6]}$ shown in the upper panel. The black dashed lines represent the 1σ region of the LHCb measurement [34], while the gray dotted lines show the boundaries of the q^2 bin where $m_X^2 = q_{\min}^2 = 1.1 \text{ GeV}^2$ and $m_X^2 = q_{\max}^2 = 6 \text{ GeV}^2$. One can clearly see that for m_X inside the bin, the minimal value of R_K is always close to the SM value $R_K^{[1,1,6]} \simeq 1$, while the corresponding value of g_X drops to zero.

To understand this behavior, it is convenient to consider the pure NP contribution proportional to $|C_9(q^2)|^2$,

$$|C_9(q^2)|^2 = \frac{q_V^2 g_X^2 (g_L^{bs})^2}{|N|^2} \frac{1}{(q^2 - m_X^2)^2 + m_X^2 \Gamma_X^2}. \quad (\text{B.11})$$

For $\Gamma_X^2 \ll m_X^2$, one can use the narrow width approximation (NWA),

$$\frac{1}{(q^2 - m_X^2)^2 + m_X^2 \Gamma_X^2} \xrightarrow{\Gamma_X^2/m_X^2 \rightarrow 0} \frac{\pi}{\Gamma_X m_X} \delta(q^2 - m_X^2), \quad (\text{B.12})$$

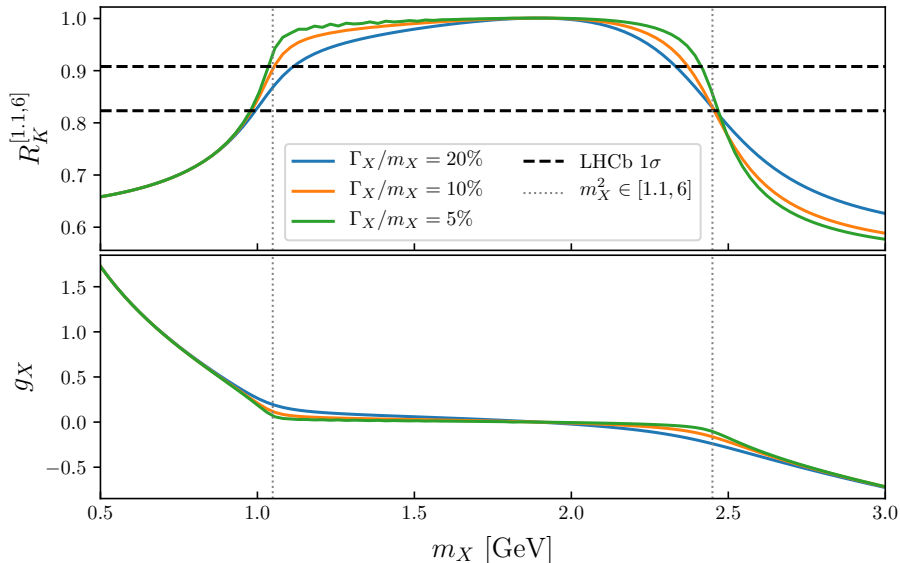


Figure 8. *Upper panel:* Minimal values of $R_K^{[1.1,6]}$ from q^2 -dependent Wilson coefficients in Eq. (B.10) with fixed $q_V = 1$, $q_A = 0$, $g_L^{bs} = 0.7 \times 10^{-8} \frac{m_X}{\text{GeV}}$ for different values of m_X and Γ_X . Blue, orange, and green lines correspond to the values obtained for a relative width Γ_X/m_X equal to 20%, 10%, and 5%, respectively. Dashed black lines correspond to the 1σ region preferred by the LHCb measurement [34]. Dotted gray lines mark the points where m_X coincides with the boundaries of the bin $q^2 \in [1.1, 6]$ GeV². *Lower panel:* Values of g_X corresponding to the minimal values of $R_K^{[1.1,6]}$ shown in the upper panel.

such that we get

$$|C_9(q^2)|^2 \Big|_{\Gamma_X^2 \ll m_X^2} \approx \frac{\pi q_V^2 g_X^2 (g_L^{bs})^2}{|N|^2 \Gamma_X m_X} \delta(q^2 - m_X^2). \quad (\text{B.13})$$

In the NWA, the δ function in the pure NP contribution dominates the integral in Eq. (B.8) if m_X^2 is inside the interval of integration. This contribution is always *positive*, so if X_μ couples to muons, the numerator of $R_{K^{(*)}}$ is always enhanced in this case. Since no suppression is possible, the minimal value of $R_K^{[1.1,6]}$ is just the SM value. At the same time, g_X has to vanish in order not to enhance $R_K^{[1.1,6]}$ even further from the experimental result. On the other hand, if m_X^2 is outside the interval of integration, the pure NP contribution vanishes in the NWA and the interference with the SM contribution can lead to a suppression of the numerator in $R_K^{[1.1,6]}$.

The effect described above is most pronounced for the narrow X_μ width and is reduced for a broad X_μ , see Fig. 8. However, even for rather wide resonances (i.e. $\Gamma_X/m_X = 20\%$), it is only possible to achieve the $R_K^{[1.1,6]}$ value preferred by the LHCb results only for m_X^2 either very close to the boundaries of the $[1.1, 6]$ GeV² bin or for m_X^2 outside this interval.

C The generators of U(1) embeddings in SU(5)

The diagonal generators of SU(5) that commute with all the generators of the conventional QCD gauge group embedding in the SU(5), $SU(3)_5 \subset SU(5)$ can be chosen as

$$T_5^{15} = \frac{1}{2\sqrt{6}} \text{diag}(1, 1, 1, -3, 0), \quad T_5^{24} = \frac{1}{2\sqrt{10}} \text{diag}(1, 1, 1, 1, -4). \quad (\text{C.1})$$

The generators of X_4 and $X_{5'}$ of $U(1)_4$ and $U(1)_{5'}$ used in section 5 are proportional to these SU(5) generators:

$$X_4 = \frac{2}{\sqrt{6}} T_5^{15} = \frac{1}{6} \text{diag}(1, 1, 1, -3, 0), \quad (\text{C.2})$$

and

$$X_{5'} = \frac{2}{\sqrt{10}} T_5^{24} = \frac{1}{10} \text{diag}(1, 1, 1, 1, -4). \quad (\text{C.3})$$

The generators X_5 of $U(1)_5$ and $X_{\mu-\tau}$ of $U(1)_{\mu-\tau}$ are given by the two linear combinations

$$X_5 = X_4 + X_{5'} = \frac{2}{15} \text{diag}(2, 2, 2, -3, -3), \quad (\text{C.4})$$

and

$$X_{\mu-\tau} = \frac{3}{2} X_4 - \frac{5}{2} X_{5'} = \text{diag}(0, 0, 0, -1, 1). \quad (\text{C.5})$$

References

- [1] A. Greljo, P. Stangl and A. E. Thomsen, *A Model of Muon Anomalies*, [2103.13991](#).
- [2] MUON G-2 collaboration, G. W. Bennett et al., *Final Report of the Muon E821 Anomalous Magnetic Moment Measurement at BNL*, *Phys. Rev. D* **73** (2006) 072003, [[hep-ex/0602035](#)].
- [3] T. Aoyama et al., *The anomalous magnetic moment of the muon in the Standard Model*, *Phys. Rept.* **887** (2020) 1–166, [[2006.04822](#)].
- [4] G. Colangelo, M. Hoferichter and P. Stoffer, *Constraints on the two-pion contribution to hadronic vacuum polarization*, *Phys. Lett. B* **814** (2021) 136073, [[2010.07943](#)].
- [5] T. Aoyama, M. Hayakawa, T. Kinoshita and M. Nio, *Complete Tenth-Order QED Contribution to the Muon $g - 2$* , *Phys. Rev. Lett.* **109** (2012) 111808, [[1205.5370](#)].
- [6] T. Aoyama, T. Kinoshita and M. Nio, *Theory of the Anomalous Magnetic Moment of the Electron*, *Atoms* **7** (2019) 28.
- [7] A. Czarnecki, W. J. Marciano and A. Vainshtein, *Refinements in electroweak contributions to the muon anomalous magnetic moment*, *Phys. Rev.* **D67** (2003) 073006, [[hep-ph/0212229](#)].
- [8] C. Gnendiger, D. Stöckinger and H. Stöckinger-Kim, *The electroweak contributions to $(g - 2)_\mu$ after the Higgs boson mass measurement*, *Phys. Rev.* **D88** (2013) 053005, [[1306.5546](#)].
- [9] M. Davier, A. Hoecker, B. Malaescu and Z. Zhang, *Reevaluation of the hadronic vacuum polarisation contributions to the Standard Model predictions of the muon $g - 2$ and $\alpha(m_Z^2)$ using newest hadronic cross-section data*, *Eur. Phys. J.* **C77** (2017) 827, [[1706.09436](#)].
- [10] A. Keshavarzi, D. Nomura and T. Teubner, *Muon $g - 2$ and $\alpha(M_Z^2)$: a new data-based analysis*, *Phys. Rev.* **D97** (2018) 114025, [[1802.02995](#)].

- [11] G. Colangelo, M. Hoferichter and P. Stoffer, *Two-pion contribution to hadronic vacuum polarization*, *JHEP* **02** (2019) 006, [[1810.00007](#)].
- [12] M. Hoferichter, B.-L. Hoid and B. Kubis, *Three-pion contribution to hadronic vacuum polarization*, *JHEP* **08** (2019) 137, [[1907.01556](#)].
- [13] M. Davier, A. Hoecker, B. Malaescu and Z. Zhang, *A new evaluation of the hadronic vacuum polarisation contributions to the muon anomalous magnetic moment and to $\alpha(\mathbf{m}_Z^2)$* , *Eur. Phys. J. C* **80** (2020) 241, [[1908.00921](#)].
- [14] A. Keshavarzi, D. Nomura and T. Teubner, *The $g - 2$ of charged leptons, $\alpha(M_Z^2)$ and the hyperfine splitting of muonium*, *Phys. Rev. D* **101** (2020) 014029, [[1911.00367](#)].
- [15] A. Kurz, T. Liu, P. Marquard and M. Steinhauser, *Hadronic contribution to the muon anomalous magnetic moment to next-to-next-to-leading order*, *Phys. Lett. B* **734** (2014) 144–147, [[1403.6400](#)].
- [16] K. Melnikov and A. Vainshtein, *Hadronic light-by-light scattering contribution to the muon anomalous magnetic moment revisited*, *Phys. Rev. D* **70** (2004) 113006, [[hep-ph/0312226](#)].
- [17] P. Masjuan and P. Sánchez-Puertas, *Pseudoscalar-pole contribution to the $(g_\mu - 2)$: a rational approach*, *Phys. Rev. D* **95** (2017) 054026, [[1701.05829](#)].
- [18] G. Colangelo, M. Hoferichter, M. Procura and P. Stoffer, *Dispersion relation for hadronic light-by-light scattering: two-pion contributions*, *JHEP* **04** (2017) 161, [[1702.07347](#)].
- [19] M. Hoferichter, B.-L. Hoid, B. Kubis, S. Leupold and S. P. Schneider, *Dispersion relation for hadronic light-by-light scattering: pion pole*, *JHEP* **10** (2018) 141, [[1808.04823](#)].
- [20] A. Gérardin, H. B. Meyer and A. Nyffeler, *Lattice calculation of the pion transition form factor with $N_f = 2 + 1$ Wilson quarks*, *Phys. Rev. D* **100** (2019) 034520, [[1903.09471](#)].
- [21] J. Bijnens, N. Hermansson-Truedsson and A. Rodríguez-Sánchez, *Short-distance constraints for the $HLbL$ contribution to the muon anomalous magnetic moment*, *Phys. Lett. B* **798** (2019) 134994, [[1908.03331](#)].
- [22] G. Colangelo, F. Hagelstein, M. Hoferichter, L. Laub and P. Stoffer, *Longitudinal short-distance constraints for the hadronic light-by-light contribution to $(g - 2)_\mu$ with large- N_c Regge models*, *JHEP* **03** (2020) 101, [[1910.13432](#)].
- [23] T. Blum, N. Christ, M. Hayakawa, T. Izubuchi, L. Jin, C. Jung et al., *The hadronic light-by-light scattering contribution to the muon anomalous magnetic moment from lattice QCD*, *Phys. Rev. Lett.* **124** (2020) 132002, [[1911.08123](#)].
- [24] G. Colangelo, M. Hoferichter, A. Nyffeler, M. Passera and P. Stoffer, *Remarks on higher-order hadronic corrections to the muon $g - 2$* , *Phys. Lett. B* **735** (2014) 90–91, [[1403.7512](#)].
- [25] S. Borsanyi et al., *Leading hadronic contribution to the muon g magnetic moment from lattice QCD*, [2002.12347](#).
- [26] LHCb collaboration, R. Aaij et al., *Measurement of CP -Averaged Observables in the $B^0 \rightarrow K^{*0} \mu^+ \mu^-$ Decay*, *Phys. Rev. Lett.* **125** (2020) 011802, [[2003.04831](#)].
- [27] LHCb collaboration, R. Aaij et al., *Angular Analysis of the $B^+ \rightarrow K^{*+} \mu^+ \mu^-$ Decay*, *Phys. Rev. Lett.* **126** (2021) 161802, [[2012.13241](#)].
- [28] LHCb collaboration, *Combination of the ATLAS, CMS and LHCb results on the $B_{(s)}^0 \rightarrow \mu^+ \mu^-$ decays*, .

- [29] LHCb collaboration, R. Aaij et al., *Differential branching fractions and isospin asymmetries of $B \rightarrow K^{(*)}\mu^+\mu^-$ decays*, *JHEP* **06** (2014) 133, [[1403.8044](#)].
- [30] LHCb collaboration, R. Aaij et al., *Angular analysis and differential branching fraction of the decay $B_s^0 \rightarrow \phi\mu^+\mu^-$* , *JHEP* **09** (2015) 179, [[1506.08777](#)].
- [31] LHCb collaboration, R. Aaij et al., *Measurements of the S-wave fraction in $B^0 \rightarrow K^+\pi^-\mu^+\mu^-$ decays and the $B^0 \rightarrow K^*(892)^0\mu^+\mu^-$ differential branching fraction*, *JHEP* **11** (2016) 047, [[1606.04731](#)].
- [32] LHCb collaboration, R. Aaij et al., *Branching fraction measurements of the rare $B_s^0 \rightarrow \phi\mu^+\mu^-$ and $B_s^0 \rightarrow f_2'(1525)\mu^+\mu^-$ decays*, [2105.14007](#).
- [33] LHCb collaboration, R. Aaij et al., *Test of lepton universality with $B^0 \rightarrow K^{*0}\ell^+\ell^-$ decays*, *JHEP* **08** (2017) 055, [[1705.05802](#)].
- [34] LHCb collaboration, R. Aaij et al., *Test of lepton universality in beauty-quark decays*, [2103.11769](#).
- [35] G. Hiller and F. Kruger, *More model-independent analysis of $b \rightarrow s$ processes*, *Phys. Rev. D* **69** (2004) 074020, [[hep-ph/0310219](#)].
- [36] M. Bordone, G. Isidori and A. Pattori, *On the Standard Model predictions for R_K and R_{K^*}* , *Eur. Phys. J. C* **76** (2016) 440, [[1605.07633](#)].
- [37] G. Isidori, S. Nabeebaccus and R. Zwicky, *QED corrections in $\bar{B} \rightarrow \bar{K}\ell^+\ell^-$ at the double-differential level*, *JHEP* **12** (2020) 104, [[2009.00929](#)].
- [38] W. Altmannshofer and P. Stangl, *New Physics in Rare B Decays after Moriond 2021*, [2103.13370](#).
- [39] L.-S. Geng, B. Grinstein, S. Jäger, S.-Y. Li, J. Martin Camalich and R.-X. Shi, *Implications of new evidence for lepton-universality violation in $b \rightarrow s\ell^+\ell^-$ decays*, [2103.12738](#).
- [40] M. Algueró, B. Capdevila, S. Descotes-Genon, J. Matias and M. Novoa-Brunet, *$b \rightarrow s\ell\ell$ global fits after Moriond 2021 results*, in *55th Rencontres de Moriond on QCD and High Energy Interactions*, 4, 2021, [2104.08921](#).
- [41] T. Hurth, F. Mahmoudi, D. M. Santos and S. Neshatpour, *More Indications for Lepton Nonuniversality in $b \rightarrow s\ell^+\ell^-$* , [2104.10058](#).
- [42] M. Ciuchini, M. Fedele, E. Franco, A. Paul, L. Silvestrini and M. Valli, *Lessons from the $B^{0,+} \rightarrow K^{*0,+}\mu^+\mu^-$ angular analyses*, *Phys. Rev. D* **103** (2021) 015030, [[2011.01212](#)].
- [43] MEG collaboration, A. M. Baldini et al., *Search for the lepton flavour violating decay $\mu^+ \rightarrow e^+\gamma$ with the full dataset of the MEG experiment*, *Eur. Phys. J. C* **76** (2016) 434, [[1605.05081](#)].
- [44] BABAR collaboration, B. Aubert et al., *Searches for Lepton Flavor Violation in the Decays $\tau_{+-} \rightarrow e_{+-}\gamma$ and $\tau_{+-} \rightarrow \mu_{+-}\gamma$* , *Phys. Rev. Lett.* **104** (2010) 021802, [[0908.2381](#)].
- [45] S. Baek, N. G. Deshpande, X. G. He and P. Ko, *Muon anomalous $g-2$ and gauged $L(\mu)$ - $L(\tau)$ models*, *Phys. Rev. D* **64** (2001) 055006, [[hep-ph/0104141](#)].
- [46] E. Ma, D. P. Roy and S. Roy, *Gauged $L(\mu)$ - $L(\tau)$ with large muon anomalous magnetic moment and the bimaximal mixing of neutrinos*, *Phys. Lett. B* **525** (2002) 101–106, [[hep-ph/0110146](#)].

- [47] K. Harigaya, T. Igari, M. M. Nojiri, M. Takeuchi and K. Tobe, *Muon $g-2$ and LHC phenomenology in the $L_\mu - L_\tau$ gauge symmetric model*, *JHEP* **03** (2014) 105, [[1311.0870](#)].
- [48] W. Altmannshofer, S. Gori, M. Pospelov and I. Yavin, *Neutrino Trident Production: A Powerful Probe of New Physics with Neutrino Beams*, *Phys. Rev. Lett.* **113** (2014) 091801, [[1406.2332](#)].
- [49] W. Altmannshofer, S. Gori, J. Martín-Albo, A. Sousa and M. Wallbank, *Neutrino Tridents at DUNE*, *Phys. Rev. D* **100** (2019) 115029, [[1902.06765](#)].
- [50] A. Crivellin, J. Fuentes-Martin, A. Greljo and G. Isidori, *Lepton Flavor Non-Universality in B decays from Dynamical Yukawas*, *Phys. Lett. B* **766** (2017) 77–85, [[1611.02703](#)].
- [51] A. Crivellin, G. D’Ambrosio and J. Heeck, *Explaining $h \rightarrow \mu^\pm \tau^\mp$, $B \rightarrow K^* \mu^+ \mu^-$ and $B \rightarrow K \mu^+ \mu^- / B \rightarrow K e^+ e^-$ in a two-Higgs-doublet model with gauged $L_\mu - L_\tau$* , *Phys. Rev. Lett.* **114** (2015) 151801, [[1501.00993](#)].
- [52] A. Crivellin, M. Hoferichter and P. Schmidt-Wellenburg, *Combined explanations of $(g-2)_{\mu,e}$ and implications for a large muon EDM*, *Phys. Rev. D* **98** (2018) 113002, [[1807.11484](#)].
- [53] W. Altmannshofer, S. Gori, M. Pospelov and I. Yavin, *Quark flavor transitions in $L_\mu - L_\tau$ models*, *Phys. Rev. D* **89** (2014) 095033, [[1403.1269](#)].
- [54] W. Altmannshofer and I. Yavin, *Predictions for lepton flavor universality violation in rare B decays in models with gauged $L_\mu - L_\tau$* , *Phys. Rev. D* **92** (2015) 075022, [[1508.07009](#)].
- [55] R. Alonso, P. Cox, C. Han and T. T. Yanagida, *Flavoured $B?L$ local symmetry and anomalous rare B decays*, *Phys. Lett. B* **774** (2017) 643–648, [[1705.03858](#)].
- [56] C. Bonilla, T. Modak, R. Srivastava and J. W. F. Valle, *$U(1)_{B_3-3L_\mu}$ gauge symmetry as a simple description of $b \rightarrow s$ anomalies*, *Phys. Rev. D* **98** (2018) 095002, [[1705.00915](#)].
- [57] B. C. Allanach, *$U(1)_{B_3-L_2}$ explanation of the neutral current B -anomalies*, *Eur. Phys. J. C* **81** (2021) 56, [[2009.02197](#)].
- [58] B. C. Allanach and J. Davighi, *Third family hypercharge model for $R_{K^{(*)}}$ and aspects of the fermion mass problem*, *JHEP* **12** (2018) 075, [[1809.01158](#)].
- [59] B. C. Allanach and J. Davighi, *Naturalising the third family hypercharge model for neutral current B -anomalies*, *Eur. Phys. J. C* **79** (2019) 908, [[1905.10327](#)].
- [60] D. Bhatia, S. Chakraborty and A. Dighe, *Neutrino mixing and R_K anomaly in $U(1)_X$ models: a bottom-up approach*, *JHEP* **03** (2017) 117, [[1701.05825](#)].
- [61] W. Altmannshofer, J. Davighi and M. Nardecchia, *Gauging the accidental symmetries of the standard model, and implications for the flavor anomalies*, *Phys. Rev. D* **101** (2020) 015004, [[1909.02021](#)].
- [62] D. Aristizabal Sierra, F. Staub and A. Vicente, *Shedding light on the $b \rightarrow s$ anomalies with a dark sector*, *Phys. Rev. D* **92** (2015) 015001, [[1503.06077](#)].
- [63] A. Celis, J. Fuentes-Martin, M. Jung and H. Serodio, *Family nonuniversal Z' models with protected flavor-changing interactions*, *Phys. Rev. D* **92** (2015) 015007, [[1505.03079](#)].
- [64] A. Falkowski, M. Nardecchia and R. Ziegler, *Lepton Flavor Non-Universality in B -meson Decays from a $U(2)$ Flavor Model*, *JHEP* **11** (2015) 173, [[1509.01249](#)].
- [65] C.-W. Chiang, X.-G. He and G. Valencia, *Z' model for $b \rightarrow s \ell \bar{\ell}$ flavor anomalies*, *Phys. Rev. D* **93** (2016) 074003, [[1601.07328](#)].

- [66] S. M. Boucenna, A. Celis, J. Fuentes-Martin, A. Vicente and J. Virto, *Non-abelian gauge extensions for B-decay anomalies*, *Phys. Lett. B* **760** (2016) 214–219, [[1604.03088](#)].
- [67] S. M. Boucenna, A. Celis, J. Fuentes-Martin, A. Vicente and J. Virto, *Phenomenology of an $SU(2) \times SU(2) \times U(1)$ model with lepton-flavour non-universality*, *JHEP* **12** (2016) 059, [[1608.01349](#)].
- [68] P. Ko, Y. Omura, Y. Shigekami and C. Yu, *LHCb anomaly and B physics in flavored Z' models with flavored Higgs doublets*, *Phys. Rev. D* **95** (2017) 115040, [[1702.08666](#)].
- [69] R. Alonso, P. Cox, C. Han and T. T. Yanagida, *Anomaly-free local horizontal symmetry and anomaly-full rare B-decays*, *Phys. Rev. D* **96** (2017) 071701, [[1704.08158](#)].
- [70] Y. Tang and Y.-L. Wu, *Flavor non-universal gauge interactions and anomalies in B-meson decays*, *Chin. Phys. C* **42** (2018) 033104, [[1705.05643](#)].
- [71] K. Fuyuto, H.-L. Li and J.-H. Yu, *Implications of hidden gauged $U(1)$ model for B anomalies*, *Phys. Rev. D* **97** (2018) 115003, [[1712.06736](#)].
- [72] L. Bian, H. M. Lee and C. B. Park, *B-meson anomalies and Higgs physics in flavored $U(1)'$ model*, *Eur. Phys. J. C* **78** (2018) 306, [[1711.08930](#)].
- [73] S. F. King, *$R_{K^{(*)}}$ and the origin of Yukawa couplings*, *JHEP* **09** (2018) 069, [[1806.06780](#)].
- [74] G. H. Duan, X. Fan, M. Frank, C. Han and J. M. Yang, *A minimal $U(1)'$ extension of MSSM in light of the B decay anomaly*, *Phys. Lett. B* **789** (2019) 54–58, [[1808.04116](#)].
- [75] I. Doršner, S. Fajfer, A. Greljo, J. F. Kamenik and N. Košnik, *Physics of leptoquarks in precision experiments and at particle colliders*, *Phys. Rept.* **641** (2016) 1–68, [[1603.04993](#)].
- [76] T. Hambye and J. Heeck, *Proton decay into charged leptons*, *Phys. Rev. Lett.* **120** (2018) 171801, [[1712.04871](#)].
- [77] J. Davighi, M. Kirk and M. Nardecchia, *Anomalies and accidental symmetries: charging the scalar leptoquark under $L_\mu - L_\tau$* , *JHEP* **12** (2020) 111, [[2007.15016](#)].
- [78] J. Wess and B. Zumino, *Consequences of anomalous Ward identities*, *Phys. Lett. B* **37** (1971) 95–97.
- [79] J. Davighi, *Anomalous Z' bosons for anomalous B decays*, [2105.06918](#).
- [80] B. C. Allanach, J. Davighi and S. Melville, *An Anomaly-free Atlas: charting the space of flavour-dependent gauged $U(1)$ extensions of the Standard Model*, *JHEP* **02** (2019) 082, [[1812.04602](#)].
- [81] K. Asai, *Predictions for the neutrino parameters in the minimal model extended by linear combination of $U(1)_{L_e-L_\mu}$, $U(1)_{L_\mu-L_\tau}$ and $U(1)_{B-L}$ gauge symmetries*, *Eur. Phys. J. C* **80** (2020) 76, [[1907.04042](#)].
- [82] T. Araki, K. Asai, J. Sato and T. Shimomura, *Low scale seesaw models for low scale $U(1)_{L_\mu-L_\tau}$ symmetry*, *Phys. Rev. D* **100** (2019) 095012, [[1909.08827](#)].
- [83] G. Hiller and M. Schmaltz, *R_K and future $b \rightarrow s\ell\ell$ physics beyond the standard model opportunities*, *Phys. Rev. D* **90** (2014) 054014, [[1408.1627](#)].
- [84] D. Buttazzo, A. Greljo, G. Isidori and D. Marzocca, *B-physics anomalies: a guide to combined explanations*, *JHEP* **11** (2017) 044, [[1706.07808](#)].
- [85] A. Crivellin, D. Müller and T. Ota, *Simultaneous explanation of $R(D^{(*)})$ and $b \rightarrow s\mu^+ \mu^-$: the last scalar leptoquarks standing*, *JHEP* **09** (2017) 040, [[1703.09226](#)].

- [86] G. Hiller and I. Nisandzic, R_K and R_{K^*} beyond the standard model, *Phys. Rev. D* **96** (2017) 035003, [[1704.05444](#)].
- [87] V. Gherardi, D. Marzocca and E. Venturini, Low-energy phenomenology of scalar leptoquarks at one-loop accuracy, *JHEP* **01** (2021) 138, [[2008.09548](#)].
- [88] A. Angelescu, D. Bečirević, D. A. Faroughy, F. Jaffredo and O. Sumensari, On the single leptoquark solutions to the B -physics anomalies, [2103.12504](#).
- [89] D. Marzocca, Addressing the B -physics anomalies in a fundamental Composite Higgs Model, *JHEP* **07** (2018) 121, [[1803.10972](#)].
- [90] I. Doršner, S. Fajfer, D. A. Faroughy and N. Košnik, The role of the S_3 GUT leptoquark in flavor universality and collider searches, *JHEP* **10** (2017) 188, [[1706.07779](#)].
- [91] K. S. Babu, P. S. B. Dev, S. Jana and A. Thapa, Unified framework for B -anomalies, muon $g - 2$ and neutrino masses, *JHEP* **03** (2021) 179, [[2009.01771](#)].
- [92] M. Bauer and M. Neubert, Minimal Leptoquark Explanation for the $R_{D^{(*)}}$, R_K , and $(g - 2)_g$ Anomalies, *Phys. Rev. Lett.* **116** (2016) 141802, [[1511.01900](#)].
- [93] I. Doršner, S. Fajfer and O. Sumensari, Muon $g - 2$ and scalar leptoquark mixing, *JHEP* **06** (2020) 089, [[1910.03877](#)].
- [94] V. Brdar, A. Greljo, J. Kopp and T. Opferkuch, The Neutrino Magnetic Moment Portal: Cosmology, Astrophysics, and Direct Detection, *JCAP* **01** (2021) 039, [[2007.15563](#)].
- [95] F. S. Queiroz and W. Shepherd, New Physics Contributions to the Muon Anomalous Magnetic Moment: A Numerical Code, *Phys. Rev. D* **89** (2014) 095024, [[1403.2309](#)].
- [96] J. M. Arnold, B. Fornal and M. B. Wise, Phenomenology of scalar leptoquarks, *Phys. Rev. D* **88** (2013) 035009, [[1304.6119](#)].
- [97] N. Assad, B. Fornal and B. Grinstein, Baryon Number and Lepton Universality Violation in Leptoquark and Diquark Models, *Phys. Lett. B* **777** (2018) 324–331, [[1708.06350](#)].
- [98] R. Barbieri, G. Isidori, A. Pattori and F. Senia, Anomalies in B -decays and $U(2)$ flavour symmetry, *Eur. Phys. J. C* **76** (2016) 67, [[1512.01560](#)].
- [99] L. Di Luzio, A. Greljo and M. Nardecchia, Gauge leptoquark as the origin of B -physics anomalies, *Phys. Rev. D* **96** (2017) 115011, [[1708.08450](#)].
- [100] A. Greljo and B. A. Stefanek, Third family quark–lepton unification at the TeV scale, *Phys. Lett. B* **782** (2018) 131–138, [[1802.04274](#)].
- [101] M. Bordone, C. Cornella, J. Fuentes-Martin and G. Isidori, A three-site gauge model for flavor hierarchies and flavor anomalies, *Phys. Lett. B* **779** (2018) 317–323, [[1712.01368](#)].
- [102] M. Bordone, C. Cornella, J. Fuentes-Martín and G. Isidori, Low-energy signatures of the PS^3 model: from B -physics anomalies to LFV, *JHEP* **10** (2018) 148, [[1805.09328](#)].
- [103] C. Cornella, J. Fuentes-Martin and G. Isidori, Revisiting the vector leptoquark explanation of the B -physics anomalies, *JHEP* **07** (2019) 168, [[1903.11517](#)].
- [104] B. Fornal, S. A. Gadam and B. Grinstein, Left-Right $SU(4)$ Vector Leptoquark Model for Flavor Anomalies, *Phys. Rev. D* **99** (2019) 055025, [[1812.01603](#)].
- [105] M. Blanke and A. Crivellin, B Meson Anomalies in a Pati-Salam Model within the Randall-Sundrum Background, *Phys. Rev. Lett.* **121** (2018) 011801, [[1801.07256](#)].

- [106] J. Fuentes-Martín, G. Isidori, M. König and N. Selimović, *Vector Leptoquarks Beyond Tree Level*, *Phys. Rev. D* **101** (2020) 035024, [[1910.13474](#)].
- [107] D. Guadagnoli, M. Reboud and P. Stangl, *The Dark Side of 4321* , *JHEP* **10** (2020) 084, [[2005.10117](#)].
- [108] J. Heeck and D. Teresi, *Pati-Salam explanations of the B-meson anomalies*, *JHEP* **12** (2018) 103, [[1808.07492](#)].
- [109] J. Fuentes-Martín and P. Stangl, *Third-family quark-lepton unification with a fundamental composite Higgs*, *Phys. Lett. B* **811** (2020) 135953, [[2004.11376](#)].
- [110] J. Fuentes-Martín, M. Reig and A. Vicente, *Strong CP problem with low-energy emergent QCD: The 4321 case*, *Phys. Rev. D* **100** (2019) 115028, [[1907.02550](#)].
- [111] J. Fuentes-Martín, G. Isidori, M. König and N. Selimović, *Vector leptoquarks beyond tree level. II. $\mathcal{O}(\alpha_s)$ corrections and radial modes*, *Phys. Rev. D* **102** (2020) 035021, [[2006.16250](#)].
- [112] J. Fuentes-Martín, G. Isidori, M. König and N. Selimović, *Vector Leptoquarks Beyond Tree Level III: Vector-like Fermions and Flavor-Changing Transitions*, *Phys. Rev. D* **102** (2020) 115015, [[2009.11296](#)].
- [113] B. A. Dobrescu and P. J. Fox, *Diophantine equations with sum of cubes and cube of sum*, [2012.04139](#).
- [114] D. B. Costa, B. A. Dobrescu and P. J. Fox, *General Solution to the $U(1)$ Anomaly Equations*, *Phys. Rev. Lett.* **123** (2019) 151601, [[1905.13729](#)].
- [115] F. Jegerlehner and A. Nyffeler, *The Muon $g-2$* , *Phys. Rept.* **477** (2009) 1–110, [[0902.3360](#)].
- [116] W. Altmannshofer, C.-Y. Chen, P. S. Bhupal Dev and A. Soni, *Lepton flavor violating Z' explanation of the muon anomalous magnetic moment*, *Phys. Lett. B* **762** (2016) 389–398, [[1607.06832](#)].
- [117] B. Abi et al., *Measurement of the Positive Muon Anomalous Magnetic Moment to 0.46 ppm*, [2104.03281](#).
- [118] MUON G-2 collaboration, T. Albahri et al., *Magnetic-field measurement and analysis for the Muon $g - 2$ Experiment at Fermilab*, *Phys. Rev. A* **103** (2021) 042208, [[2104.03201](#)].
- [119] MUON G-2 collaboration, T. Albahri et al., *Measurement of the anomalous precession frequency of the muon in the Fermilab Muon $g - 2$ Experiment*, *Phys. Rev. D* **103** (2021) 072002, [[2104.03247](#)].
- [120] A. Crivellin, M. Hoferichter, C. A. Manzari and M. Montull, *Hadronic Vacuum Polarization: $(g - 2)_\mu$ versus Global Electroweak Fits*, *Phys. Rev. Lett.* **125** (2020) 091801, [[2003.04886](#)].
- [121] A. Keshavarzi, W. J. Marciano, M. Passera and A. Sirlin, *Muon $g - 2$ and $\Delta\alpha$ connection*, *Phys. Rev. D* **102** (2020) 033002, [[2006.12666](#)].
- [122] R. Jackiw and S. Weinberg, *Weak interaction corrections to the muon magnetic moment and to muonic atom energy levels*, *Phys. Rev. D* **5** (1972) 2396–2398.
- [123] CCFR collaboration, S. R. Mishra et al., *Neutrino tridents and $W Z$ interference*, *Phys. Rev. Lett.* **66** (1991) 3117–3120.
- [124] G. Bellini et al., *Precision measurement of the ${}^7\text{Be}$ solar neutrino interaction rate in Borexino*, *Phys. Rev. Lett.* **107** (2011) 141302, [[1104.1816](#)].

- [125] BOREXINO collaboration, M. Agostini et al., *First Simultaneous Precision Spectroscopy of pp, ${}^7\text{Be}$, and pep Solar Neutrinos with Borexino Phase-II*, *Phys. Rev. D* **100** (2019) 082004, [[1707.09279](#)].
- [126] P. Ilten, Y. Soreq, M. Williams and W. Xue, *Serendipity in dark photon searches*, *JHEP* **06** (2018) 004, [[1801.04847](#)].
- [127] M. Bauer, P. Foldenauer and J. Jaeckel, *Hunting All the Hidden Photons*, *JHEP* **07** (2018) 094, [[1803.05466](#)].
- [128] G. Krnjaic, G. Marques-Tavares, D. Redigolo and K. Tobioka, *Probing Muonphilic Force Carriers and Dark Matter at Kaon Factories*, *Phys. Rev. Lett.* **124** (2020) 041802, [[1902.07715](#)].
- [129] NA62 collaboration, E. Cortina Gil et al., *Search for K^+ decays to a muon and invisible particles*, *Phys. Lett. B* **816** (2021) 136259, [[2101.12304](#)].
- [130] BABAR collaboration, J. P. Lees et al., *Search for a muonic dark force at BABAR*, *Phys. Rev. D* **94** (2016) 011102, [[1606.03501](#)].
- [131] P. Ilten, Y. Soreq, J. Thaler, M. Williams and W. Xue, *Proposed Inclusive Dark Photon Search at LHCb*, *Phys. Rev. Lett.* **116** (2016) 251803, [[1603.08926](#)].
- [132] LHCb collaboration, R. Aaij et al., *Search for Dark Photons Produced in 13 TeV pp Collisions*, *Phys. Rev. Lett.* **120** (2018) 061801, [[1710.02867](#)].
- [133] LHCb collaboration, R. Aaij et al., *Search for $A' \rightarrow \mu^+ \mu^-$ Decays*, *Phys. Rev. Lett.* **124** (2020) 041801, [[1910.06926](#)].
- [134] D. Banerjee et al., *Dark matter search in missing energy events with NA64*, *Phys. Rev. Lett.* **123** (2019) 121801, [[1906.00176](#)].
- [135] BABAR collaboration, J. P. Lees et al., *Search for a Dark Photon in e^+e^- Collisions at BaBar*, *Phys. Rev. Lett.* **113** (2014) 201801, [[1406.2980](#)].
- [136] NA62 collaboration, E. Cortina Gil et al., *Search for production of an invisible dark photon in π^0 decays*, *JHEP* **05** (2019) 182, [[1903.08767](#)].
- [137] C.-Y. Chen, J. Kozaczuk and Y.-M. Zhong, *Exploring leptophilic dark matter with NA64- μ* , *JHEP* **10** (2018) 154, [[1807.03790](#)].
- [138] B. Batell, N. Lange, D. McKeen, M. Pospelov and A. Ritz, *Muon anomalous magnetic moment through the leptonic Higgs portal*, *Phys. Rev. D* **95** (2017) 075003, [[1606.04943](#)].
- [139] S. N. Gninenko, N. V. Krasnikov and V. A. Matveev, *Muon $g-2$ and searches for a new leptophobic sub-GeV dark boson in a missing-energy experiment at CERN*, *Phys. Rev. D* **91** (2015) 095015, [[1412.1400](#)].
- [140] NA64 collaboration, D. Banerjee et al., *Search for invisible decays of sub-GeV dark photons in missing-energy events at the CERN SPS*, *Phys. Rev. Lett.* **118** (2017) 011802, [[1610.02988](#)].
- [141] Y. Kahn, G. Krnjaic, N. Tran and A. Whitbeck, *M^{β} : a new muon missing momentum experiment to probe $(g-2)_{\mu}$ and dark matter at Fermilab*, *JHEP* **09** (2018) 153, [[1804.03144](#)].
- [142] Y. Jho, Y. Kwon, S. C. Park and P.-Y. Tseng, *Search for muon-philic new light gauge boson at Belle II*, *JHEP* **10** (2019) 168, [[1904.13053](#)].

- [143] I. Galon, E. Kajamovitz, D. Shih, Y. Soreq and S. Tarem, *Searching for muonic forces with the ATLAS detector*, *Phys. Rev. D* **101** (2020) 011701, [[1906.09272](#)].
- [144] A. Kamada, K. Kaneta, K. Yanagi and H.-B. Yu, *Self-interacting dark matter and muon $g - 2$ in a gauged $U(1)_{L_\mu - L_\tau}$ model*, *JHEP* **06** (2018) 117, [[1805.00651](#)].
- [145] D. Croon, G. Elor, R. K. Leane and S. D. McDermott, *Supernova Muons: New Constraints on Z' Bosons, Axions and ALPs*, *JHEP* **01** (2021) 107, [[2006.13942](#)].
- [146] N. Bar, K. Blum and G. D'Amico, *Is there a supernova bound on axions?*, *Phys. Rev. D* **101** (2020) 123025, [[1907.05020](#)].
- [147] F. Sala and D. M. Straub, *A New Light Particle in B Decays?*, *Phys. Lett. B* **774** (2017) 205–209, [[1704.06188](#)].
- [148] BELLE-II collaboration, F. Abudinén et al., *Search for $B^+ \rightarrow K^+ \nu \bar{\nu}$ decays using an inclusive tagging method at Belle II*, [2104.12624](#).
- [149] BELLE collaboration, J. Grygier et al., *Search for $B \rightarrow h \nu \bar{\nu}$ decays with semileptonic tagging at Belle*, *Phys. Rev. D* **96** (2017) 091101, [[1702.03224](#)].
- [150] BABAR collaboration, J. P. Lees et al., *Search for $B \rightarrow K^{(*)} \nu \bar{\nu}$ and invisible quarkonium decays*, *Phys. Rev. D* **87** (2013) 112005, [[1303.7465](#)].
- [151] BELLE collaboration, O. Lutz et al., *Search for $B \rightarrow h^{(*)} \nu \bar{\nu}$ with the full Belle $\Upsilon(4S)$ data sample*, *Phys. Rev. D* **87** (2013) 111103, [[1303.3719](#)].
- [152] K. Hayasaka et al., *Search for Lepton Flavor Violating Tau Decays into Three Leptons with 719 Million Produced Tau+Tau- Pairs*, *Phys. Lett. B* **687** (2010) 139–143, [[1001.3221](#)].
- [153] D. W. P. d. Amaral, D. G. Cerdeno, P. Foldenauer and E. Reid, *Solar neutrino probes of the muon anomalous magnetic moment in the gauged $U(1)_{L_\mu - L_\tau}$* , *JHEP* **12** (2020) 155, [[2006.11225](#)].
- [154] S. Weinberg, *Models of Lepton and Quark Masses*, *Phys. Rev. D* **101** (2020) 035020, [[2001.06582](#)].
- [155] M. J. Baker, P. Cox and R. R. Volkas, *Has the Origin of the Third-Family Fermion Masses been Determined?*, *JHEP* **04** (2021) 151, [[2012.10458](#)].
- [156] M. J. Baker, P. Cox and R. R. Volkas, *Radiative muon mass models and $(g - 2)_\mu$* , *JHEP* **05** (2021) 174, [[2103.13401](#)].
- [157] ATLAS collaboration, G. Aad et al., *Search for pairs of scalar leptoquarks decaying into quarks and electrons or muons in $\sqrt{s} = 13$ TeV pp collisions with the ATLAS detector*, *JHEP* **10** (2020) 112, [[2006.05872](#)].
- [158] ATLAS collaboration, *Search for pair production of scalar leptoquarks decaying to first or second generation leptons and boosted hadronically decaying top quarks in pp collisions at $\sqrt{s} = 13$ TeV with the ATLAS detector*, .
- [159] C. Poole and A. E. Thomsen, *Constraints on 3- and 4-loop β -functions in a general four-dimensional Quantum Field Theory*, *JHEP* **09** (2019) 055, [[1906.04625](#)].